FOSSIL ENERGY

DOE/BC/14126-13

(DE89000767)

PHASE CHANGE IN BINARY SYSTEMS IN POROUS MEDIA: APPLICATION TO SOLUTION GAS DRIVE

By

Yanis C. Yortsos

Mehmet Parlar

October 1989

Performed Under Contract No. FG19-87BC14126

University of Southern California

Los Angeles, California

Bartlesville Project Office
U. S. DEPARTMENT OF ENERGY
Bartlesville, Oklahoma

This report has been reproduced directly from the best available copy.

Available to DOE and DOE contractors from the Office Of Scientific and Technical Information, P.O. Box 62, Oak Ridge, TN 37831; prices available from (615)576-8401, FTS 626-8401.

Available to the public from the National Technical Information Service, U.S. Department of Commerce, 5285 Port Royal Rd., Springfield, VA 22161

Price: Printed A04
Microfiche A01

DOE/BC/14126-13

Distribution Category UC-122

PHASE CHANGE IN BINARY SYSTEMS IN POROUS MEDIA: APPLICATION TO SOLUTION GAS DRIVE

By

Yanis C. Yortsos

Mehmet Parlar

October 1989

Work Performed Under Contract No. FG19-87BC14126

Prepared for

U. S. Department of Energy

Assistant Secretary for Fossil Energy

Thomas B. Reid, Project Manager

Bartlesville Project Office

P. O. Box 1398

Bartlesville, OK 74005

Prepared by

University of Southern California

Los Angeles, CA 90089-1211

TABLE OF CONTENTS

PAGE

Abstract 1
Introduction 2
Nucleation 5
Bubble Growth 12
Percolation Theory at Low Supersaturations 23
Conclusions 26
Nomenclature 28
References 31
Appendix A 35
Appendix B 38
Table 1 40

FIGURES

Figure 1a. Gas solubility vs. pressure schematic 41

Figure 1b. Typical solution gas-oil ratio vs. pressure 42

Figure 2a. Schematic of a nucleation site in a host pore body 43

Figure 2b. Schematic of bubble radius-volume relationship 44

Figure 3a. Nucleation fraction at threshold vs. β ($Z = 6$) 45

Figure 3b. Pore body and pore throat size distributions 46

Figure 4a. Critical supersaturation vs. f for various decline rates: $a = 1(U)$, $a = 10^{-4}$ psi/sec (L) 47

Figure 4b. Critical supersaturation vs. pressure decline rate for $f = 0.1$ 48

Figure 5. Schematic of a gas bubble in a porous medium 49

Figure 6. Critical gas saturation for various nucleation fractions 50

Figure 7. Critical gas saturation as a function of β ($\kappa = 0.1$) 51

Figure 8a. Internal (A,B) and external (C) gas drive relative permeabilities, $\beta = 0.20, 0.16, 0$, respectively ($Z = 6$) 52

Figure 8b. Internal gas drive relative permeabilities ($Z = 6$, $\beta = 0.09$, $\kappa = 0.1$) 53

PHASE CHANGE IN BINARY SYSTEMS IN POROUS MEDIA: APPLICATION TO SOLUTION GAS-DRIVE

By

Y.C. Yortsos and M. Parlar

ABSTRACT

In this paper, a study of the liquid-to-vapor phase change by pressure decline in porous media is presented. A simplified solution gas drive system is taken as a representative example. The issues of nucleation, critical supersaturation, and vapor phase growth in porous media are critically examined. At low supersaturations a percolation approach is proposed that allows for the estimation of critical gas saturation and relative permeabilities from nucleation and pore structure characteristics.

INTRODUCTION

Processes involving phase change in porous media are routinely encountered in numerous applications. The liquid-to-gas transition, in particular, is common to applications such as geothermal systems, thermal methods for oil recovery, solution gas-drive reservoirs and cavitation. With few exceptions, these phenomena have been treated on a phenomenological basis, where the important roles of the microstructure of the porous medium are largely ignored. And while there is wide recognition of the fundamental differences between internal and external drives, surprisingly little has been published to quantify such effects.

The change of phase in porous media is described by the two consecutive processes of nucleation and phase growth. For the porous media of interest to us, the nucleation mechanism is fundamentally identical to common nucleation, with due emphasis to heterogeneous nucleation (although see also Ref. [1] for phase transitions in tight porous media).

Bubble growth, on the other hand, is controlled by the pore wall curvature and geometry that may stabilize otherwise unstable gas bubbles. This is a basic difference to bubble growth in the bulk, a process studied in great detail since the pioneering works by Plesset and Zwick,[2] and Scriven.[3] Additional parameters of importance in porous media involve the critical gas saturation, and the effect of imposed supersaturation (pressure decline or superheat in solution gas-drive or boiling) on the growth pattern of the gas phase. The geometry and topology of the porous medium constrain the growth of the new phase and pose novel problems.

In general, vapor-bubble dynamics are classified into two broad categories:[4] one involving vapor-bubble growth due to a reduction of the liquid pressure (sometimes to negative values, as in the case of homogeneous cavitation), and another involving vapor growth in a superheated liquid, corresponding to boiling. The two processes are physically similar in many respects: In addition to common inertia, viscous and surface forces, bubble growth is controlled by diffusion of the volatile species in the first case, and by diffusion (conduction) of heat in the latter. In this paper, however, our emphasis will be on the pressure reduction in a binary

mixture consisting of a volatile (solution gas) and a non-volatile (oil) component, and we shall defer the analysis of boiling to a future study.

The body of literature on nucleation and bubble growth in bulk liquids is immense. A very selective and subjective review of relevant works will be briefly summarized here. The state of the art in homogeneous nucleation is reviewed by Binder[5] with emphasis on Monte-Carlo methods. From an engineering viewpoint, phase transitions are elucidated by Springer.[6] Heterogeneous nucleation is reviewed by Cole[7] who summarized the original ideas by Fisher[8] and Bankoff[9] in the context of boiling, and by Crum[10] in the context of cavitation. Additional contributions to heterogeneous nucleation were made by Ward and Forest,[11] and by Forest[12] for a binary system, the homogeneous nucleation of which was first presented by Ward et al.[13] The reduction of the vapor pressure of the less volatile component (Kelvin equation) and the nuclei stability were thoroughly analysed. The homogeneous nucleation of multi-component mixtures was reviewed by Blander and Katz,[14] and by Thome and Shock.[15] Effects of phase behavior in reducing the effective supersaturation were also highlighted.

Bubble growth in supersaturated systems has been treated in the seminal work by Scriven,[3] where diffusive effects are considered in the absence of inertia, viscous and surface forces. Closed-form asymptotic solutions are obtained for the growth of bubbles in the bulk. The growth of an isolated spherical bubble by solute diffusion was numerically studied in the important papers by Szekely and Martins,[16] and by Szekely and Fang.[17] These authors provide a comparative study of the significance of inertia, viscous, mass transfer, and non-equilibria effects in bubble growth.

A useful review of bubble dynamics in general, with emphasis on cavitation was presented by Plesset and Prosperetti.[4] These authors addressed in a subsequent publication[18] vapor growth in a superheated liquid. The various asymptotic, perturbation and approximate techniques in bubble growth and their domain of applicability were systematically appraised by Vrentas and Shin.[19,20] Significantly fewer are studies in the growth of a population of bubbles, where various size bubbles compete for a fixed mass of solute through diffusion. We cite the work by

Engelking[21] who applied coarsening ideas by Lifshitz and Slyozov[22] as also confirmed by Marqusee and Ross,[23] to infer that initially broad population densities asymptotically peak to a single- (large) size distribution.

In sharp contrast, the literature on phase change and bubble growth in porous media is substantially leaner. Early experimental studies on nucleation focused, rather inconclusively, on the effect of the rate of pressure decline.[24–27] Similar experiments using glass micromodels were recently reported.[28] Theoretical issues of nucleation in the liquid-to-vapor transition in porous media were addressed in recent studies by Parlar and Yortsos,[29] and by Hirasaki et al.,[30] in the contexts of vapor desorption and cavitation in a capillary centrifuge. Both works emphasize the importance of heterogeneous nucleation in porous media. Parlar and Yortsos[29] also proposed a quantitative nucleation model for estimating nucleation fractions.

Fundamental studies on the subsequent growth of the vapor phase are also sparse. The early literature reports on laboratory experiments that attempt to simulate a solution gas-drive process. The importance of diffusion was singled out by Handy.[31] Visualization experiments were reported by Chatenever et al.,[32] and by Dumore,[33] while an attempt to analyze the process was undertaken by Abgrall and Iffly.[34] The latter work, as well as that of Epstein[35] in the context of inertia-controlled bubble growth, essentially treat the porous medium as an equivalent "bulk" system, with limited regard due to the microgeometry. Bubble growth controlled by capillarity was considered in recent studies by Parlar and Yortsos[29,36] on capillary desorption.

It must be apparent from the above brief review that the issues of phase change and vapor-bubble growth in a porous medium are far from being sufficiently explored. In view of the routine occurrence of such phenomena, an investigation of their basic features would be a worthwhile undertaking. This is the main objective of the paper. As previously noted, we shall consider the phase change in the context of the solution gas-drive process, which for our purposes will be taken to consist of a liquid phase containing a volatile and a non-volatile species, and a gas phase containing the volatile component. The process is driven by a pressure decline below the "bubble point", P_b, of the mixture to the value P_∞. We shall examine

the response of the system, namely nucleation and bubble growth, to the imposed supersaturation $\Delta P = P_b - P_\infty$.

By necessity, the paper is presented in two parts, one on nucleation and the other on the subsequent gas-phase growth. The part on nucleation addresses issues of heterogeneous nucleation, the stability of nuclei in cavities along the pore walls, issues of nucleation rates and critical supersaturation. The part on phase growth is a study of the dominant processes summarized in terms of dimensionless parameters. Inertia, viscous, capillary and mass transfer effects are discussed in terms of the imposed supersaturation. Equilibrium states and their stability are investigated. We identify the pertinent regimes appropriate to specific cases and the associated growth patterns. In the limit of quasi-static growth at low supersaturations, analytical expressions are proposed for critical gas saturation and gas relative permeabilities in terms of the structural characteristics of the porous medium.

NUCLEATION

The basic ideas underlying nucleation are common to any phase change. Here we shall briefly summarize essentials of nucleation theories in the context of liquid-to-vapor transition, which we will subsequently apply to the solution gas drive process in porous media.

Current homogeneous nucleation theories rely on the theory of fluctuations for the formation of critical size nuclei (embryos).[5] This is a modern extension of the phenomenological approach,[6,7] which uses traditional thermodynamics and kinetics to determine equilibrium sizes, their stability, and rates of formation. As an example, we consider (metastable) equilibrium gas bubbles in the bulk of a liquid containing two species, only one of which (component 1) is volatile. Thermodynamic (mechanical and chemical) equilibrium defines the radius of curvature of the gas bubble[37]

$$P_V = P_L + \frac{2\gamma}{r} \tag{1}$$

$$r = \frac{2\gamma}{KC - P_L} \tag{2}$$

where P_V and P_L are the pressures in the gas and the liquid, respectively, and K is the solubility constant (see also below). For a fixed concentration C of the volatile species, (2) relates uniquely the equilibrium radius to the liquid pressure. The above is also valid for any equilibrium vapor-liquid interface including those in a cavity (typical of heterogeneous nucleation). When component 2 is slightly volatile, a similar expression can be also derived,[13] that generalizes Kelvin's equation.

Gas Solubility

Implicit in the above derivation is the use of linear phase relations. Phase equilibria across a flat interface between a liquid and its vapor are in general quite complex. For simplicity, we shall postulate a linear relationship between the concentration of the volatile component (solution gas) at equilibrium, C_{sat}, and the liquid pressure, the latter being equal to the pressure of the vapor when the interface is flat

$$P_L = KC_{sat} \tag{3}$$

It follows that $P_b = KC_\infty$. A given pressure supersaturation ΔP may then be translated into an equivalent concentration supersaturation $\Delta C = C_\infty - C_o$ (Fig. 1a). Although various laws based on an "ideal solution", such as Raoult's or Henry's laws, and typical gas-oil ratio curves (Figure 1b) can be invoked to justify this approximation, we shall refrain from doing so, particularly since for small supersaturations, a linear relationship between pressure and concentration increments can always be assumed. Of course, the approximation can be severe for large supersaturations.

A more important issue in our context is the value of K, which for the system of Fig. 1b, was estimated to be of the order of 3.75×10^4 psi/gr/cc. The latter value was obtained by using the arbitrary ratio of 6 between the molecular weights of solution and solute and taking the liquid density to be 0.8 gr/cc. Substantially

more refined methods for phase equilibria can of course be used for an accurate estimate of the solubility constant K and its variation.

Nucleation Rates

An important issue relevant to nucleation is the rate of generation of critical nuclei. In the case of homogeneous nucleation, classical kinetic theories can be used with relative success to predict the formation rate

$$J = \frac{dN}{dt} = \frac{N_o k_B T \rho_L \phi}{hM} \exp(-\frac{\Delta F}{k_B T}) \tag{4}$$

where $\Delta F = 4\pi\gamma r_c^2/3$ is the free energy to form the equilibrium nucleus, k_B and h the Boltzmann and Planck constants, respectively, and N_o is the Avogadro number. For heterogeneous nucleation, two approaches have been proposed, both of which rely on the existence of surface heterogeneities or nucleation sites (e.g., conical cavities) that are not liquid-wet. The most popular approach postulates that such sites contain pre-existing (or trapped) vapor, provided that certain requirements on the conical and contact angles are met.[10] In such a case, the issue of rate of nuclei formation is non-existent and the condition for nucleation is obtained by directly applying (2), with the radius of curvature evaluated as the conical pit mouth radius W (Figure 2a)

$$KC - P_L = \frac{2\gamma}{W} \tag{5}$$

The other approach parallels homogeneous nucleation in that pre-existing vapor is not required, although surface sites with the desired wettability and geometry must exist.[7] A nucleation rate expression similar to (4) is conjectured

$$J = \frac{dN}{dt} = K_{het} \exp(-\frac{\Delta F}{k_B T} f) \tag{6}$$

where K_{het} is a kinetic constant,[8] and f is a function of site geometry and wettability, ranging between 1 and 0 in the limits of homogeneous and perfect heterogeneous nucleation, respectively. Equation (6) can then be used to calculate the

nucleation pressure, or the critical supersaturation, usually defined by arbitrarily assuming $J = 1$ nucleus/sec-cc

$$r_N = \left(\frac{3k_B T \ln K_{het}}{4\pi\gamma f}\right)^{1/2} \tag{7}$$

The precise value assigned to J or K_{het} is immaterial.[38] For example, for the homogeneous nucleation of a liquid with molecular weight 100 and density 0.7 g/cc at 200 °F, the change of J from 1 to 10^8 reduces the nucleation radius from 21.7 to 19 Angstrom, clearly a negligible change.

Nucleation in Porous Media

During a liquid-to-gas transition in porous media, the occupancy of pores by the gas phase occurs either through access to bulk vapor (as in external gas/steam drive) or through a nucleation process inside the pores. The question arises, therefore, as to what nucleation mechanisms would be typically expected in a porous material.

Homogeneous nucleation can be discounted, since it requires the drastic conditions of absence of impurities, perfectly smooth and liquid wet solid surfaces, and no trapped gases. Moreover, as previously pointed out the nucleation radius for homogeneous nucleation is of the order of a few nm, with corresponding supersaturations of several thousand psi. Thus, unless the pore sizes are of the same order, homogeneous nucleation can be disregarded as a mechanism for bubble formation.

The selection of heterogeneous nucleation as the dominant mechanism drastically reduces the critical supersaturation, as interfaces of large radius of curvature can form in surface cavities, given the proper wettability conditions. Unfortunately, additional simplifications are necessary, if a quantitative model is to be further developed.

We proceed by representing the surface roughness by uniform wettability conical cavities, among which only the largest one needs to be considered. The contact

angle in the cavity may take any nonzero, but preferably high, value while complete wetting by liquid is assumed in the main pore body (Figure 2a). Using elementary geometry, the volume of the bubble can be related to the radius of the gas-liquid interface. Figure 2b qualitatively portrays such a relationship for a hydrophilic cavity ($\theta - \alpha < \pi/2$), that satisfies the relation $W/r < \cos(\theta - \alpha)$. Hydrophobic cavities were considered by Hirasaki et al.[30] To proceed further, we will assume that a self-similarity exists between the maximum size cavity and the size of the host pore body. Thus, the ratio $\beta = W/r$ will be taken constant. In the absence of additional information, this assumption is a reasonable one. Although the ensuing results are subject to this premise, most of the expressions obtained are also independently valid.

Consider now the nucleation process in a conical cavity, with curvature corresponding to the equilibrium value given by (5). The stability of mechanical equilibrium in gas-liquid interfaces in cavities was examined by various authors.[11,12,30] A quite general result is obtained: mechanically stable interfaces ($d^2\Delta F/dV_G^2 > 0$) require configurations such that $dr/dV < 0$, while mechanically unstable interfaces ($d^2\Delta F/dV_G^2 < 0$) correspond to $dr/dV > 0$. Thus, for the hydrophilic cavity shown in Figure 2a the gas-liquid interface is unstable within the cavity, but becomes stabilized at the pit mouth. Similar conclusions are drawn for the hydrophobic cavities with pre-existing vapor (where, now, the interface is stable inside the cavity as well). In both cases, the pit mouth radius W is the smallest possible radius for a stable equilibrium interface to exist in the cavity. Hence, W dictates the critical supersaturation (5), beyond which the pore body is substantially filled with vapor. It follows that the occupancy of a pore body via nucleation would occur at a specific supersaturation corresponding to (5) and, thus, be uniquely correlated to the pore body size, if the assumption on β is retained.

The fraction of pores that would nucleate (nucleation fraction) at a radius r_d corresponding to a given supersaturation (5) is thus

$$f_q = b\frac{\int_{r_d/\beta}^{\infty} \alpha_s(r)dr}{\int_{r_d}^{\infty} \alpha_s(r)dr} \tag{8}$$

A constant b can also be introduced to allow favorable wettability conditions only for a fraction of such pits. This expression is needed for the evaluation of the accessibility functions[29,36] that were derived independent of the distribution of cavity sizes. Figure 3a shows the relationship between β and f_q for b = 1 and for the pore body size distributions shown in Figure 3b. Relatively small values of f_q are obtained for small β for the particular distributions taken. This model will later be used to calculate critical gas saturations and relative permeabilities.

Pressure Decline Rate

The effect of pressure decline rate on the critical supersaturation has been pursued by several investigators. In the absence of issues other than strict nucleation, an estimate of its effect can be directly obtained from the above analysis. For the present purposes, we shall define critical supersaturation as that necessary for the occupancy of a single (or a few) pore(s) with gas, although we are aware of other definitions that have also been used in the literature. If pre-existing vapor exists in hydrophobic conical cavities, the activation of the latter is almost instantaneous as soon as the proper supersaturation is applied, thus no effect of pressure decline rate should be observed. The possibility of some effect may exist, in the case of hydrophilic cavities with no initially trapped vapor. A simple analysis, however, indicates that the effect is negligible.

Assuming that the nucleation rate expression (6) is applicable,

$$\frac{dN}{dt} = K_{het} \exp[-\frac{\lambda}{(\Delta P)^2}] \tag{9}$$

where $\lambda = 16\pi\gamma^3 f/(3k_B T)$. For a pressure decline rate of the form $\Delta P = at$, an integration of (9) yields

$$\frac{aN}{K_{het}\sqrt{\lambda}} = \frac{1}{x}\exp(-x^2) - \sqrt{\pi}\mathrm{erfc}(x) \tag{10}$$

where $x = \sqrt{\lambda}/\Delta P$. The solution of (10) for $N = 1$ (arbitrarily selected but without loss in generality, as pointed out above) is shown in Figure 4 for various

values of the wettability parameter f and the decline rate a. It is noted that, although the effect of f is very significant (Figure 4a), as indeed expected, the pressure decline rate has a negligible influence on the supersaturation, even for variations spanning 5 orders of magnitude (Figure 4b). One concludes that the critical supersaturation required for nucleation is a property of the liquid and the porous medium, and practically independent of external parameters.

Pore Body Occupancy

Upon establishment of the critical supersaturation, the bubble interface becomes mechanically unstable, thus growth occurs until the bubble radius reaches the pore body size (or detaches from the pit). Further growth results into a decreasing radius of curvature, due to the converging pore walls, and such configurations will be stable, if they would also happen to correspond to the equilibrium curvature as specified by the existing supersaturation. As shown in a later section, such interfaces are also stable to mass transfer. If the supersaturation is too large, invasion of surrounding pores by vapor will ensue, until an appropriate stabilizing pore geometry is encountered. It is worthwhile to stress this important characteristic of porous media, namely the stabilization of otherwise (in the bulk) unstable interfaces.

As a closing note we demarcate the conditions necessary for the bubble not to detach from the cavity, before it grows to the pore body size. We shall balance surface and gravity forces to obtain

$$r < \left(\frac{3\beta c_t}{4}\frac{\gamma}{\rho_L g}\right)^{1/2} \tag{11}$$

where c_t is a cavity perimeter constant, equal to 2 for a flat surface. For the values of Table 1, a pore size r greater than about 400 microns is required in order for gravity-induced detachment to be of concern.

BUBBLE GROWTH

The preceding section described the conditions for the occupancy by the vapor phase of one (or a few connected) pore bodies. In the next part, the study of the growth of the vapor phase is undertaken. For convenience, an isolated "bubble" is first, considered. An extension to a population of bubbles is discussed for a special case in a later section.

Single Bubble in Porous Medium

We shall consider the growth of a single vapor bubble occupying a small part of an infinitely large porous medium, the rest of which is filled with liquid (Figure 5). For the present purposes, other nucleation events are suppressed, and we need not specify in detail the conditions for the existence of the initial bubble. From its definition, the bubble is connected, although not necessarily spherical (although individual interface menisci are spherical). A supersaturation $\Delta P = P_b - P_\infty$, in general variable with time, but for the moment considered fixed, is assumed to apply far from the bubble. The system is taken "infinitely large" so that the solute concentration far from the bubble, C_∞, is constant and equal to the solubility at pressure P_b.

Equilibrium States

Preceding an analysis of growth, the study of possible equilibrium states is required. The question posed is whether a gas bubble can exist in a porous medium in stable equilibrium with a supersaturated liquid. It is well known that a vapor bubble in an unbounded bulk liquid is in unstable mechanical equilibrium and will either grow indefinitely or collapse. Under the premise of chemical equilibrium, the stability of gas-liquid interfaces in the presence of constraining surfaces has been examined, as discussed in the nucleation part above. Those predictions imply that an equilibrium gas bubble located such that its mean curvature lies between the smallest pore body curvature (largest radius) and the smallest pore

throat curvature (largest radius) associated with that pore body, is stable. Here, we shall also consider the stability of the interface to mass transfer.

We take a gas bubble in equilibrium, occupying volume V_o, at pressure P_{vo} and containing n_o moles. Concentration and pressure in the liquid are spatially uniform and equal to C_∞ and P_∞, respectively. Ideal gas conditions and linear phase equilibria dictate

$$KC_\infty V_o = n_o RT \tag{12}$$

where R is the ideal gas constant, while mechanical equilibrium at the gas-liquid interface requires spherical-shape menisci of constant mean curvature H_o

$$KC_\infty - P_\infty = 2\gamma H_o \tag{13}$$

Since the RHS in the above measures the capillary pressure of the porous medium, the present analysis is effectively meaningful only for low supersaturations. Equilibrium states at high supersaturations correspond to almost complete occupancy by the gas phase (with the possible exception of thin films). Although conditions of low supersaturation are certainly violated in typical laboratory experiments, they are more likely to be satisfied in a typical field case, where pressure decline rates on the order of psi/day or less may be common. The mathematical analysis of stability is based on linearization and is described in Appendix A. Here we shall provide a simple physical interpretation of the results obtained.

Consider small perturbations in the curvature of an equilibrium vapor-liquid meniscus located in a converging pore element (pore body to pore throat). Under the assumption of a constant liquid pressure and fast kinetics at the interface, an increase (decrease) in curvature implies a corresponding increase (decrease) in gas pressure, thus, an increase (decrease) in the concentration at the interface. A concentration gradient in the liquid phase develops that leads to a solute mass flux away from (towards) the interface, hence to a reduction (increase) in the gas phase volume. For a converging pore element, the latter implies a restoration of the initial curvature, thus stability. In the opposite case of a diverging pore, the mass

transfer compounds the disturbance, and at least to first order, the equilibrium state is unstable.

Similar arguments also apply in the case where the gas phase surrounds a liquid "drop" and the liquid can escape through thin films. There, the liquid pressure may be taken constant and the previous approach is applicable. In the absence of thin films, however, the liquid compressibility becomes important. The decrease in liquid volume upon advancement of the interface results into a substantial increase in liquid pressure. When the curvature also increases (as is the case in converging pores), a concomitant increase in gas pressure and interface concentration follow, giving rise to the previous mass transfer argument. Again, such interfaces are stable to mass transfer. In the case of interfaces in diverging pores, there is a decrease in the interfacial curvature. The concomitant change in the gas phase pressure, however, is expected to be positive

$$\frac{dP_V}{dH} = (\gamma - \frac{dV_L/dH}{V_L c_p}) < 0 \tag{14}$$

due to the small liquid compressibility, c_p, which easily counterbalances capillary effects. A higher interface concentration follows, thus leading to a stabilizing effect. Therefore, in the absence of communication with the bulk, equilibrium gas-liquid interfaces surrounding liquid droplets are stable to mass transfer, regardless of the particular volume-curvature relationship.

Bubble Growth

The growth of a vapor bubble in a porous medium is controlled by forces similar to those in the bulk, namely inertia, viscous, surface and pressure. Supersaturation in the liquid drives the process, while the specific pore geometry of the porous medium constrains the growth pattern obtained. We shall, first, study growth due to a supersaturation ΔC, brought about by an imposed step change in the liquid pressure, ΔP. Following Szekely and Martins,[16] we shall characterize the growth process in terms of suitable dimensionless groups. Typical parameter values used are listed in Table 1.

Dimensionless Groups

Denoting by H_o a reference mean curvature of the menisci of the initial bubble, we define the key dimensionless parameter

$$\Phi = \frac{2\gamma H_o}{\Delta P} \tag{15}$$

Small supersaturations are comparable to surface forces and lead to O(1) or greater values in Φ, while large supersaturations correspond to $\Phi \ll 1$. In the present illustrations, the smallest value that Φ can attain is 10^{-5} (for $\Delta P \approx 2000$ psia). A dimensionless expression for the driving force for bubble growth is the Jacob number

$$\mathrm{Ja} = \frac{\Delta C}{\rho_G(P_\infty)} \tag{16}$$

which can be also expressed in terms of Φ by use of (15) and the ideal gas law

$$\mathrm{Ja} = \frac{2\gamma R T H_o}{K M_1 P_\infty} \frac{1}{\Phi} \tag{17}$$

For relatively small supersaturations, $\Delta P \ll P_\infty$, we take $P_\infty \approx 2000$ psia, so that at these conditions the reference Jacob number is (Table 1)

$$\mathrm{Ja} = \frac{10^{-4}}{\Phi} \tag{18}$$

Thus, for a small supersaturation, Ja is considerably less than O(1). On the other hand, for moderate and large supersaturations, P_∞ can be significantly small and Ja may reach values as high as 20000 (when P_∞ is O(1 psia)), or even higher at conditions of vacuum. Although Ja indicates the direction of growth, an additional useful indicator is the measure of diffusion vs. inertia effects expressed through the parameter

$$B = \frac{\mathrm{Ja}^2}{\sqrt{G}} \tag{19}$$

where

$$G = \frac{R_o^2 \Delta P}{\rho_L D^2} \tag{20}$$

and R_o is the "bubble radius". According to Szekely and Martins,[16] $B \ll 1$ signifies mass transfer (diffusion) control, while $B \gg 1$ denotes inertia-controlled process. In our case, a conservative estimate of B yields

$$B = 10^{-5} \mathrm{Ja}^2 \Phi^{1/2} \tag{21}$$

For small supersaturations, $B \ll 1$ and the process is clearly mass transfer controlled. Inertia control may set in the process only under severe conditions, most likely requiring application of vacuum. For example, even for a sharp reduction of P_∞ to 1 atm, the estimated value of B is only O(1). Although atypical for a field case, processes with not small B may be used in laboratory experiments.

Significant other parameters are the Schmidt number of the liquid phase

$$\mathrm{Sc} = \frac{\mu}{\rho D} \approx 1.25 \times 10^4 \tag{22}$$

indicating fast momentum transfer compared to mass transfer, and a modified capillary number

$$N_{ca} = \frac{\mu D}{\gamma R_o} \approx 10^{-5} \tag{23}$$

In the above, mass transfer control has been assumed in estimating liquid velocities and the "bubble radius" was conservatively approximated by 50 μm. We expect smaller values for N_{ca} when the bubble size is larger and when the supersaturation is smaller. In the latter case one may use a different time scale instead (see also below)

$$N_{ca} = \frac{\mu D}{\gamma R_o} \mathrm{Ja}^2 \tag{24}$$

which, for small Ja, unequivocally establishes capillary control in the momentum balance.

Bubble Growth Regimes

In discussing the growth of gas bubbles we shall proceed in order of increasing complexity from low to high supersaturations.

A. Low Supersaturations, $\Delta P \ll P_\infty$

We consider a small step reduction ΔP of the initial liquid pressure P_b to the value P_∞, which is still large for condition $\Delta P \ll P_\infty$ to be valid. This should be the case for field operations at low pressure decline rates (see also below). At these conditions, the growth process is mass transfer-controlled, inertia and viscous forces are negligible, and the solution density may be considered constant in the diffusion equation. The relevant equations in dimensional notation read as follows. In the pore space occupied by the liquid, one has

$$\frac{\partial C}{\partial t} + \underline{u} \cdot \nabla C = D \nabla^2 C \tag{25}$$

$$\nabla \cdot \underline{u} = 0 \tag{26}$$

The gas phase is taken at spatially constant pressure P_V and has volume V_o. Denoting by A the gas-liquid interface (which excludes possible thin films), a mass balance at the interface gives

$$\rho_G \underline{u} \cdot \underline{s} = D \nabla C \cdot \underline{s} \tag{27}$$

and in integrated form

$$\frac{d}{dt}[V \rho_G] = D \int_A \underline{s} \cdot \nabla C dA \tag{28}$$

where $\underline{s}$ is the outwards pointing (from gas-to-liquid) normal. Ideal gas conditions, linear phase behavior and the Laplace equation complete the description

$$\rho_G = \frac{P_V M_1}{RT} \tag{29}$$

$$P_V = KC\,|_A \tag{30}$$

$$P_V = P_\infty + 2\gamma H \tag{31}$$

where H is the mean curvature at the gas-liquid boundary, assumed prescribed by the pore geometry. The latter equation represents the momentum balance with negligible inertia and viscous effects. Boundary and initial conditions

$$\begin{aligned} C &\to C_\infty \quad \text{at} \quad \underline{r} \to \infty \\ \underline{u} &\to 0 \quad \text{at} \quad \underline{r} \to \infty \\ C &= C_\infty \quad \text{at} \quad t = 0 \end{aligned} \tag{32}$$

along with a specification of the initial "bubble" configuration are also needed.

The above system is, of course, too complex to be solved by simple methods. Fortunately, additional simplifications can be made with an appropriate dimensionless formulation. We scale spatial distance by an initial "bubble radius" R_o, time by $R_o^2/D\mathrm{Ja}$, velocity by $D\mathrm{Ja}/R_o$, bubble volume by R_o^3, interfacial area by R_o^2, and interfacial curvature by H_o (which is generally unrelated to R_o). We further define dimensionless concentration and gas pressure

$$\Sigma = \frac{C - C_o}{\Delta C} \tag{33}$$

$$\Pi = \frac{P_V - P_\infty}{\Delta P} \tag{34}$$

to obtain

$$\mathrm{Ja}\left(\frac{\partial \Sigma}{\partial \tau} + \underline{\nu} \cdot \nabla \Sigma\right) = \nabla^2 \Sigma \tag{35}$$

$$\nabla \cdot \underline{\nu} = 0 \tag{36}$$

$$\Sigma = 1 \quad \text{at } \infty \text{ and at } \tau = 0 \tag{37}$$

where the nomenclature is self-evident, $\underline{\nu}$ being the dimensionless velocity, while at the gas-liquid interface we have

$$\nu_s = \frac{\partial \Sigma}{\partial s} \tag{38}$$

$$\Pi = \Sigma \tag{39}$$

$$\Pi = \Phi\eta \tag{40}$$

where η is the dimensionless curvature. Finally, the growth of the dimensionless volume $\Upsilon = V/R_o^3$ satisfies the equation

$$\frac{d}{d\tau}[\Upsilon(1+\Pi\frac{\Delta P}{P_\infty})] = \int_A \frac{\partial\Sigma}{\partial s}dA \tag{41}$$

which, in our case of low supersaturation, becomes

$$\frac{d\Upsilon}{d\tau} = \int_A \frac{\partial\Sigma}{\partial s}dA \tag{42}$$

It must be noted that the above dimensionless formulation was chosen so as to balance rates of growth with diffusion. It is then apparent that as long as $\Delta P/P_\infty$ is small, then Ja $\ll 1$, and the mass transfer equation becomes

$$\nabla^2\Sigma = 0 \tag{43}$$

implying that the concentration field is quasi-static. The quasi-static approximation is widely used in mass transfer involving growing phases at low supersaturations (e.g., Lifshitz and Slyozov[22]), it has been vigorously derived by Scriven[3] and confirmed numerically by Szekely and Martins,[16] and other authors in various contexts.

The emergence of a quasi-static concentration field has a significant impact on the method of solution of the problem. Indeed, we shall show that our problem is mathematically equivalent to that of immiscible displacement, where a low viscosity gas injected at a source, immiscibly displaces an incompressible liquid of constant far-field pressure. A dimensionless formulation of the problem is presented in Appendix B. Direct comparison of (B-8)–(B-12) with (37)–(43) shows that the two formulations are identical under the equivalence

$$\Sigma \leftrightarrow \Lambda \quad \text{and} \quad \Phi \leftrightarrow \Psi \tag{44}$$

The immiscible displacement from a single source described in Appendix B results into various growth patterns depending on the relative importance of capillarity. When capillary forces predominate, the displacement is a percolation process, equilibrium states will be reached at the specified capillary pressure, and the associated patterns are well known (in either ordinary or invasion percolation). On the other hand, when viscous forces predominate, the displacement is of the DLA type, no equilibrium states are possible and the growth pattern is determined solely by the solution of the Laplace equation in the liquid.

Therefore, in view of the equivalence (44) we may then conjecture that at low supersaturations, the growth of the gas bubble is as follows:

(i) When $\Phi \sim O(1)$, i.e., $2\gamma H_o \sim \Delta P \ll P_\infty$, the process is (invasion) percolation, the properties of which have been extensively studied in recent years.[39] For a given ΔP satisfying the above, the bubble evolves towards an equilibrium percolation pattern, dictated by capillarity. It is apparent from (38–40), that the final pattern corresponds to $\eta = 1/\Phi$, $(\Sigma = 1)$. In conjunction with the stability of equilibrium states discussed above, simple rules for the occupancy of the pore space by gas can be constructed: Pores with small and allowed curvature $\eta < 1/\Phi$, $(R > 2\gamma/\Delta P)$ are occupied by gas, provided that they are accessible to the initial bubble. Predictions on critical gas saturation and relative permeabilities for this classical percolation problem are presented in a later section.

However, it should be cautioned that, although the final pattern is fixed, the rate of approach may be quite slow, as is also the case in similar capillary invasion processes,[40] and may depend significantly on the size of the gas bubble before supersaturation was applied. An order of magnitude estimate for the dimensional time to equilibrium is

$$t_{eq} \sim \frac{k\xi^2}{\phi D \mathrm{Ja}^2} \tag{45}$$

where k is the medium permeability (that scales pore length) and ξ is the dimensionless correlation length in the percolation process. The latter is generally O(1) away from the percolation threshold (i.e. at low and high gas saturation), but in-

creases sharply near percolation (i.e. near the critical gas saturation). Although further research is certainly needed for definitive answers, the above can be used to provide plausible estimates on the range of pressure decline rates, where the above percolation regime is applicable. A practical approach is to approximate the continuous pressure decline as a sequence of quasi-static, small ΔP steps, and to ensure that sufficient time has been allotted for equilibrium. For a pressure decline rate a, a characteristic time $t^* = \Delta P/a$ is defined. We shall demand $t^* \gg t_{eq}$, hence

$$a \ll \frac{\phi \Delta P D}{k\xi^2} \mathrm{Ja}^2 \tag{46}$$

Taking $\Phi \sim O(1)$, $\xi \sim O(1)$, and using (18), the above yields a typical estimate of $a \ll 10^{-4}$ psi/sec, far from percolation, which is quite realistic for field cases. Of course, near the threshold, the diffusion process slows down considerably, and even lower decline rates are required for the percolation regime to be applicable.

(ii) <u>When $\Phi \ll 1$</u>, i.e., $2\gamma H_o \ll \Delta P \ll P_\infty$, the process is diffusion-limited, capillarity is unimportant, and the growth pattern should be of the DLA (Diffusion-Limited-Aggregation) type. Here, with the possible exception of trapped liquid, equilibrium states do not exist other than full occupancy of the medium by gas. Indeed, for $\Phi \ll 1$, equations (39), (40) give $\Sigma = 0$ at the gas-liquid interface, which in view of the far-field boundary condition $\Sigma = 1$ and (41) imply continuous growth. The growth pattern resembles that in viscous-controlled, immiscible displacement with unfavorable mobility ratio ($\mathrm{Ca} \gg 1$, $M_m \gg 1$), a process recently studied by a DLA approach.[41] The gas-occupied pore space is a fractal object of fixed fractal dimension. Evidently, in such cases the use of classical concepts such as relative permeabilities and critical gas saturation is inappropriate, although alternative methods have yet to be developed.

Processes with Φ values intermediate between the two extremes identified in (i) and (ii), are naturally more complex, and our understanding of the displacement properties is poor, at present. Likewise incomplete is our knowledge of processes with rapid enough pressure decline rate a, such that the above constraint (46) is violated. In conjunction with other topics outlined below, these issues call for

further research.

B. Moderate Supersaturations, $\Delta P \sim P_\infty$

When the supersaturation step ΔP is comparable to the imposed liquid pressure P_∞ , surface forces are negligible in the momentum balance, ($\Phi \ll 1$), and inertia and viscous forces may still be neglected ($B \ll 1$). Thus, the process is, again, mass transfer-controlled, although now Ja $\sim O(1)$. Equations (25),(26) of the previous section still describe the growth, although a modification to account for liquid density changes must also be considered. Even in the absence of the latter, however, the problem is quite complex, since the quasi-static approximation (43) is no longer valid when Ja is not small. Here the full diffusion-convection equation (25) must be considered, which is further coupled with the flow field in the liquid. The solution to this complex problem is beyond the scope of this paper.

C. Large Supersaturations, $\Delta P \gg P_\infty$

We conclude this part by noting that at large supersaturations, inertia and viscous effects previously ignored, acquire importance at the early stages of bubble growth, under conditions such that $B \gg 1$. Examination of (21) reveals that the latter condition demands high ΔP, low P_∞ (possibly vacuum) and low K (high gas solubility). In inertia-controlled growth the mass of gas in the bubble remains constant, and the bubble expands following a polytropic law.[4] A first attempt to the solution of this problem in porous media was undertaken by Epstein.[35] However, here too, the state of the art is quite unsatisfactory and in need of additional work.

D. Growth from Multiple Source Sites

A final remark is necessary concerning the growth of gas bubbles that originate from more than one nucleation sites. Our treatment of nucleation specifies that nucleation sites at various pore bodies are instantly activated when the local supersaturation reaches a threshold value characterizing the pore body. Thus, the possibility of growth from several sources is a real issue and must be addressed. In the next section, we present a solution to this problem for the case of low

supersaturations or pressure decline rates, when capillarity predominates (case A(i) above). A modification of percolation theory is implemented to account for growth from multiple sites. Unfortunately, the same cannot be done for any other case which are in need of further work. Finally, an application of the present study to finite systems which are closed to mass transfer should have an interest of its own. In such cases, growth, solute depletion, activation of nucleation sites and "bubble coalescence" occur simultaneously and the underlying competition should share features common to those studied by Lifshitz and Slyozov.[22] It must be remarked that several reported experiments operate under the constraints of finite solute mass.

PERCOLATION THEORY AT LOW SUPERSATURATIONS

It was pointed out above that at small supersaturations, induced by a low pressure decline rate, a quasi-static approximation applies. Gas phase occupancy is controlled by the capillary properties of the porous medium and can be simulated reasonably well with a percolation approach. Since nucleation must also be allowed, the usual percolation approach must be modified to account for generation at appropriate sites. Such a modification to ordinary percolation was recently presented for capillary desorption processes in Bethe lattices.[29,36] Here, we shall follow an identical approach, although invasion percolation (that accounts for a finite compressibility of the trapped liquid) yields probably a better description. However, the ensuing errors are small, if the gas saturations are not too high, and negligible if the liquid can escape through thin films.

A network representation of the porous medium in terms of a Bethe lattice is taken. Although lacking the reconnection properties of regular networks (such as a cubic), Bethe lattices allow for closed-form solutions and yield reasonable approximations to real lattice properties, such as accessibility, provided that the percolation thresholds are matched. For reasons, previously outlined in detail, both site and bond (pore body and pore throat) distributions are considered. The rules for occupancy of the pore space by the gas phase are described in [29] and can be briefly summarized as follows: Given a supersaturation $\Delta P = P_b - P_\infty$,

pore bodies with size

$$r \geq r_d = \frac{2\gamma}{\Delta P} \tag{47}$$

are allowed to be occupied. Those that are actually occupied, however, must be connected through occupied pore elements to source (nucleation) sites. Nucleation sites consist of all pore bodies with size

$$r \geq \frac{r_d}{\beta} = \frac{2\gamma}{\beta \Delta P} \tag{48}$$

where β is a fraction, assumed small ($\beta < 1$). Along with appropriate probability densities and the accessibility expressions derived in [29], [36] the above rules are sufficient for a complete description of the process. We shall illustrate the determination of the critical gas saturation as a function of β, or equivalently the nucleation fraction f_q. Gas-phase relative permeability curves will also be derived.

Critical Gas Saturation

To determine the critical gas saturation, we consider the supersaturation ΔP_c corresponding to a value r_{dc} such that the allowed bond fraction is equal to the percolation threshold, p_c

$$\int_{r_{dc}}^{\infty} \alpha_b(r) dr = p_c = \frac{1}{Z-1} \tag{49}$$

It must be noted that it is bond percolation that dictates connectivity, hence the bond distribution is used. Thus, the supersaturation ΔP_c at the onset of gas flow

$$\Delta P_c = \frac{2\gamma}{r_{dc}} \tag{50}$$

where r_{dc} solves (49), is fixed for fixed Z and $\alpha_b(r)$. Higher values in the coordination number and larger throat sizes (permeability) yield correspondingly lower

critical supersaturation. The critical gas saturation S_{gc}, is obtained by adding the volumetric contributions of the pore elements associated with the infinitely-connected bonds (those on the percolation cluster) to those connected to nucleation sites that happen not to belong on the percolation cluster. For example, the number fraction of such sites (termed *accessible*) is given by

$$X_{s,o} = q^* - (1 - f_q)[(\frac{1-p}{1-x})^Z - (1-p)^Z] + (q - q^*)f_q \tag{51}$$

where

$$q = \int_{r_d}^{\infty} \alpha_s(r)dr \quad \text{and} \quad q^* = 1 - (1-p)^Z \tag{52}$$

and x solves

$$x(1-x)^{Z-2} = (1 - f_q)p(1-p)^{Z-2} \tag{53}$$

The corresponding saturation can then be directly obtained. Results are shown in Figure 6. We note that S_{gc} crucially depends on the nucleation fraction (equivalently on β), ranging from zero, in the absence of nucleation, to values as large as

$$S_{gc} = 1 - (1 - p_c)^Z \tag{54}$$

A precise determination, of course, requires among other input the accurate allotment of volume to occupied sites and bonds, as well as their respective distributions. These parameters should vary among the various porous media. For instance, some interesting results arise when a finite maximum cutoff in the body size distribution is taken, such that the ratio $\kappa = r_{dc}/r_{s,max}$ is not identically zero. Depending on the position of β relative to this ratio, S_{gc} displays different sensitivity (Figure 7). Values of β to the left of κ correspond to cases such that although conditions for bond percolation exist, gas phase occupancy has not occurred because of lack of nucleation sites. When the first (or first few) such site(s)

is (are) created (at $r_d = \beta r_{s,max}$) the infinite cluster corresponding to that value would eventually become occupied and takes on a relatively large value.

Relative Permeabilities

Given pore element occupancies the associated relative permeability curves can also be constructed. The approach was pioneered by Heiba et al.[42] and applied to a single component steam-water system by Parlar and Yortsos,[43] where a detailed account of the technical issues is given. Drainage relative permeability pairs corresponding to internal gas drive are shown in Figure 8a for different values of β. It is evident that the difference in the curves between internal and external drive is reflected by a difference in β, thus nucleation. For $S_{gc} \approx 0$, the difference between the two processes is negligible. As nucleation events increase (and $\beta > \kappa$), S_{gc} increases, and the curve shifts to the left. The effect can become as pronounced as allowed by the magnitude of S_{gc}. Note that in these cases, $k_{rg}(S_{gc}) = 0$, while for $S_g < S_{gc}$, $k_{rg} = 0$ and $k_{rL} < 1$.

On the other hand, when nucleation effects are suppressed ($\beta < \kappa$), there is a sudden appearance of a flowing gas phase saturation, and the relative permeability curve k_{rg} practically coincides with that of an external drive, with the exception of course that it commences at S_{gc} (Fig. 8b). Besides the obvious exceptions, the relative permeability to liquid is not significantly affected and remains approximately the same in either internal or external drive.

CONCLUSIONS

In this paper a study of the basic mechanisms involved in solution-gas drive and other related liquid-to-vapor transitions in porous media was initiated. The principal issues of nucleation, supersaturation and gas-phase growth were examined. A simple geometric model was presented for heterogeneous nucleation on the pore walls which was shown to be the dominant nucleation mechanism. It was, thereby, concluded that, for otherwise identical conditions, nucleation events are likely to

occur in the larger pore bodies first, and that the supersaturation needed for the appearance of the first bubble should be largely independent of features unrelated to the porous media nature (such as, for example, the rate of pressure decline).

A detailed study of the phenomena involved in the growth of a single gas bubble in an unbounded porous medium was next considered. The effects of capillarity, mass transfer, inertia and viscous stresses were discussed. It was shown that at small supersaturations, stable equilibrium gas bubbles in converging pore elements are possible. Complementing the stability to mechanical equilibrium, stability to mass transfer was demonstrated. This is an essential requirement for the validity of the quasi-static, percolation approach at low supersaturations.

The gas-phase growth was parametrized by various dimensionless groups and the $\Delta P/P_\infty$ ratio. For small values of the latter, it was shown that the process is mass transfer-controlled, and the concentration field is quasi-static. When capillary effects dominate, ($\Phi >> 1$) the process was mapped to (invasion) percolation, while in the opposite case ($\Phi << 1$) the identification with a DLA-like process was suggested. For larger values of the ratio, the process is still mass transfer-controlled, although the diffusion is not quasi-static any longer. Inertia, viscous and density effects at large supersaturations were discussed but not explored. Issues of activation of additional nucleation sites, competition in growth and a finite supply were identified as important, but likewise were not explored.

Limiting constraints on the pressure decline rate for the quasi-static percolation approach to be valid were derived. Based on the latter, a mechanistic model was developed that accounted for growth from multiple source sites. The critical gas saturation, S_{gc}, was obtained and shown to depend crucially on the nucleation characteristics (taken here as a geometrical input) of the porous medium. Relative permeability curves pertaining to internal gas drive were also developed. Related issues for higher supersaturations were not, however, discussed. The investigation highlighted the challenging issues associated with phase transition and growth in porous media and identified areas for future research. Processes, such as solution-gas drive, cavitation and boiling in porous media would be the beneficiaries of such future advances.

NOMENCLATURE

a = pressure decline rate

A = area

B = dimensionless parameter (Eq. 19)

c_p = liquid compressibility

c_t = perimeter constant

C = concentration

Ca = capillary number

D = diffusion coefficient

f = nucleation site wettability-geometry function

f_q = nucleation fraction

G = dimensionless parameter (Eq. 20)

F = Helmholtz function

h = Planck constant

H = mean curvature

J = nucleation rate

Ja = Jacob number

k = permeability

k_B = Boltzmann constant

k_r = relative permeability

K = solubility constant

K_{het} = heterogeneous nucleation kinetic constant

M = molecular weight

M_m = mobility ratio

n = number of moles

N_o = Avogadro's number

N_{ca} = modified capillary number

p = allowed fraction of pore throats

p_c = percolation threshold

P = pressure

q = allowed fraction of pore bodies

q^* = associated fraction

r = radius

R = ideal gas constant

R_o = initial bubble radius

S = saturation

Sc = Schmidt number

t = time

T = temperature

u = velocity

V = volume

W = pit radius

$X_{s,o}$ = accessible fraction of pore bodies

Z = coordination number (connectivity)

Greek

α = half pit angle

α_b = pore throat size distribution function

α_s = pore body size distribution function

β = pit to pore body size ratio

γ = interfacial tension

η = dimensionless curvature

θ = contact angle

κ = percolation to maximum pore-body radius ratio

Λ = dimensionless liquid pressure

μ = viscosity

ν = dimensionless velocity

ξ = dimensionless correlation length

Π = dimensionless gas pressure

ρ = density

Σ = dimensionless concentration

τ = dimensionless time

Υ = dimensionless volume

ϕ = porosity

Φ = dimensionless parameter (Eq. 15)

Ψ = dimensionless parameter (Eq. B-11)

Subscripts

L = liquid

V (G) = vapor (gas)

1 = light component

REFERENCES

1. Goh, M.C., Goldburg, W.I., and Knobler, C.M.: "Phase Separation of a Binary Liquid Mixture in a Porous Medium," *Phys. Rev. Lett.* **58** (1987) 1008-1011.

2. Plesset, M.S. and Zwick, S.A.: "The Growth of Vapor Bubbles in Superheated Liquids," *J. Appl. Phys.* **25** (1954) 493-500.

3. Scriven, L.E.: "On the Dynamics of Phase Growth," *Chem. Eng. Sci.* **10** (1959) 1-13.

4. Plesset, M.S. and Prosperetti, A.: "Bubble Dynamics and Cavitation," *Ann. Rev. Fluid Mech.* **9** (1977) 145-185.

5. Binder, K.: "Theory of First-Order Phase Transitions," *Rep. Prog. Phys.* **50** (1987) 783-859.

6. Springer, G.S.: "Homogeneous Nucleation," *Adv. Heat Trans.* **14** (1978) 281-346.

7. Cole, R.: "Boiling Nucleation," *Adv. Heat Trans.* **10** (1974) 85-166.

8. Fisher, J.C.: "The Fracture of Liquids," *J. Appl. Phys.* **19** (1948) 1062-1067.

9. Bankoff, S.G.: "Ebullition from Solid Surfaces in the Absence of a Pre-Existing Gaseous Phase," *Trans. ASME* (May 1957) 735-740.

10. Crum, L.A.: "Nucleation and Stabilization of Microbubbles in Liquids," *Appl. Sci. Res.* **38** (1982) 101-115.

11. Ward, C.A. and Forest, T.W.: "On the Relation Between Platelet Adhesion and the Roughness of a Synthetic Biomaterial," *Ann. Biomed. Eng.* **4** (1976) 184-207.

12. Forest, T.W.: "The Stability of Gaseous Nuclei at Liquid-Solid Interfaces," *J. Appl. Phys.* **53** (1982) 6191-6201.

13. Ward, C.A., Balakrishnan, A., and Hooper, F.C.: "On the Thermodynamics of Nucleation in Weak Gas-Liquid Solutions," *Trans. ASME* **92** (1970) 695-704.

14. Blander, M. and Katz, J.L.: "Bubble Nucleation in Liquids," *AIChE J.* **21** (1975) 833-848.

15. Thome, J.R. and Shock, R.A.W.: "Boiling of Multicomponent Liquid Mixtures," *Adv. Heat Trans.* **16** (1980) 60-153.

16. Szekely, J. and Martins, G.P.: "Non-equilibrium Effects in the Growth of Spherical Gas Bubbles due to Solute Diffusion," *Chem. Eng. Sci.* **26** (1971) 147-159.

17. Szekely, J. and Fang, S.D.: "Non-equilibrium Effects in the Growth of Spherical Gas Bubbles due to Solute Diffusion-II: The Combined Effects of Viscosity, Liquid Inertia, Surface Tension, and Surface Kinetics," *Chem. Eng. Sci.* **28** (1973) 2127-2140.

18. Prosperetti, A. and Plesset, M.S.: "Vapour Bubble Growth in a Superheated Liquid," *J. Fluid Mech.* **85** (1978) 349-368.

19. Vrentas, J.S. and Shin, D.: "Perturbation Solutions of Spherical Moving Boundary Problems-I: Slow Growth or Dissolution Rates," *Chem. Eng. Sci.* **35** (1980) 1687-1696.

20. Vrentas, J.S. and Shin, D.: "Perturbation Solutions of Spherical Moving Boundary Problems-II: Rapid Growth or Dissolution Rates," *Chem. Eng. Sci.* **35** (1980) 1697-1705.

21. Engelking, P.C.: "Lifetimes of Metastable Microbubbles," *J. Phys. Chem.* **89** (1985) 1520-1523.

22. Lifshitz, I.M. and Slyozov, V.V.: "The Kinetics of Precipitation from Supersaturated Solid Solutions," *J. Phys. Chem. Solids* **19** (1961) 35-50.

23. Marqusee, J.A. and Ross, J.: "Kinetics of Phase Transitions: Theory of Ostwald Ripening," *J. Chem. Phys.* **79** (1983) 373-378.

24. Kennedy, H.T. and Olson, C.R.: "Bubble Formation in Supersaturated Hydrocarbon Mixtures," *Trans. AIME* **195** (1952) 271-278.

25. Stewart, C.R., Hunt Jr., E.B., Schneider, F.N., Geffen, T.M., and Berry Jr., V.J.: "The Role of Bubble Formation in Oil Recovery by Solution Gas Drives in Limestones," *Trans. AIME* **201** (1954) 294-301.

26. Hunt Jr., E.B., and Berry Jr., V.J.: "Evolution of Gas from Liquids Flowing through Porous Media," *AIChE J* **2** (1956) 560-567.

27. Wieland, D.R. and Kennedy, H.T.: "Measurement of Bubble Frequency in Cores," *Trans. AIME* **210** (1957) 122-125.

28. Danesh, A., Peden, J.M., Krinis, D., and Henderson, G.D.: "Pore Level Visual Investigation of Oil Recovery by solution Gas Drive and Gas Injection," paper *SPE 16956* presented at the 62nd Annual Meeting of SPE, Dallas, TX, Sept. 27-30, 1987.

29. Parlar, M. and Yortsos, Y.C.: "Nucleation and Pore Geometry Effects on Capillary Desorption Processes in Porous Media," *J. Coll. Intf. Sci.*, in press.

30. Hirasaki, G.J., O'Meara Jr., D.J., and Rohan, J.A.: "Centrifuge Measurements of Capillary Pressure: Part 2 - Cavitation," paper *SPE 18592* presented at the 63rd Annual Meeting of SPE, Houston, TX, Oct. 2-5, 1988.

31. Handy, L.L.: "A Laboratory Study of Oil Recovery by Solution Gas Drive," *Trans. AIME* **213** (1958) 310-315.

32. Chatenever, A., Indra, M.K., and Kyte, J.R.: "Microscopic Observations of Solution Gas Drive Behavior," *JPT* (June 1959) 13-15.

33. Dumore, J.M.: "Development of Gas Saturation During Solution Gas Drive in an Oil Layer Below a Gas Cap," *SPEJ* (Sept 1970) 211-218.

34. Abgrall, E. and Iffly, R.: "Physical Study of Flows by Expansion of Dissolved Gas," *Rev. IFP* (Sept.-Oct. 1973) 667-692 (in French).

35. Epstein, D.: "Expansion of a High-Pressure Gas Sphere in a Highly Porous Medium," *J. Geophys. Res.* **72** (1967) 3701-3710.

36. Parlar, M. and Yortsos, Y.C.: "Percolation Theory of Vapor Adsorption-Desorption Processes in Porous Materials," *J. Coll. Intf. Sci.* **124** (1988) 162-176.

37. Parlar, M., *Ph.D. Thesis*, University of Southern California, Los Angeles, CA, 1989.

38. Adamson, A.W.: *Physical Chemistry of Surfaces*, Wiley, New York, 1982.

39. Wilkinson, D. and Willemsen, J.F.: "Invasion Percolation: A New Form of Percolation Theory," *J. Phys. A: Math. Gen.* **16** (1983) 3365-3376.

40. Thompson, A.H., Katz, A.J., and Krohn, C.E.: "The Microgeometry and Transport Properties of Sedimentary Rock," *Adv. Phys.* **36** (1987) 625-694.

41. Feder, J.: *Fractals*, Plenum, New York, 1988.

42. Heiba, A.A., Sahimi, M., Scriven, L.E., and Davis, H.T.: "Percolation Theory of Two-Phase Relative Permeability," paper *SPE 11015* presented at the 57th Annual Meeting of SPE, New Orleans, LA, Sept. 26-29, 1982.

43. Parlar, M. and Yortsos, Y.C.: "Percolation Theory of Steam-Water Relative Permeability," paper *SPE 16969* presented at the 62nd Annual Meeting of SPE, Dallas, TX, Sept. 27-30, 1987.

44. Craft, B.C. and Hawkins, M.F.:*Applied Petroleum Reservoir Engineering*, Prentice-Hall, Englewood Cliffs, 1959.

APPENDIX A

Consider small disturbances from the equilibrium state of Figure 5. Neglecting second order effects associated with convection in the liquid, and changes in the liquid density, the solute concentration satisfies the diffusion equation

$$\frac{\partial C}{\partial t} = \nabla^2 C \quad \text{in liquid} \tag{A-1}$$

The assumptions of ideal gas law and linear phase equilibria at the gas-liquid interface are applicable

$$C_s = \frac{nRT}{KV} \tag{A-2}$$

$$C = C_s \quad \text{at interface} \tag{A-3}$$

A mole balance on the volatile component at the liquid-vapor interface yields

$$\frac{dn}{dt} = \frac{D}{M_1} \int_A \underline{s} \cdot \nabla C \mid_A dA \tag{A-4}$$

where A denotes the vapor-liquid interface, $\underline{s}$ is the outer normal vector. Finally, the momentum balance where inertia effects are secondary and viscous terms are insignificant yields

$$\frac{nRT}{V} = P_\infty + 2\gamma H \tag{A-5}$$

It must be stressed that snap-off events are not considered here. The formulation of the linearized problem is completed by specifying a volume-curvature geometric relationship

$$V = V(H) \tag{A-6}$$

the far region boundary condition

$$C \to C_\infty \tag{A-7}$$

and by linearizing around the equilibrium given by Eqs. (12)-(13). Denoting disturbances by prime, one obtains a diffusion equation for C' and the interface condition

$$C' = \frac{2\gamma H'}{K} \tag{A-8}$$

$$\frac{d}{dt}[\frac{2\gamma V_o H'}{RT} + \frac{KC_\infty}{RT}V'] = \frac{D}{M_1}\int_{A_o} \underline{s}\cdot\nabla C' \mid_{A_o} dA \tag{A-9}$$

where the surface integral is over A_o, the original interface, since mass fluxes from the incremental area are second order. The geometric relationship $V(H)$ is a basic ingredient of our analysis as it reflects the pore wall geometry. We linearize

$$V = V(H) = V(H_o) + H'\dot{V}(H_o) + \cdots \tag{A-10}$$

thus

$$V' = H'\dot{V}(H_o) \tag{A-11}$$

where dot denotes derivative with respect to the argument. Dimensionless notation is next introduced by denoting

$$\sigma = \frac{C'}{C_\infty},\ \tau = \frac{tD}{l^2},\ \eta = 2H'l,\ \mathcal{V} = \frac{V'}{l^3},\ \mathcal{A} = \frac{A_o}{l^2}$$

where l is to be defined shortly. One obtains the system

$$\frac{\partial\sigma}{\partial\tau} = \nabla^2\sigma \tag{A-12}$$

$$\sigma = 0 \text{ at } \infty \text{ and at } \tau = 0 \tag{A-13}$$

$$\sigma = N_1\eta \quad \text{at interface} \tag{A-14}$$

$$N\frac{d\eta}{d\tau} = \int_{\mathcal{A}} \underline{s}\cdot\nabla\sigma \mid_{\mathcal{A}} dA \quad \text{at interface} \tag{A-15}$$

$$\underline{s}\cdot\nabla\sigma = 0 \quad \text{at pore walls} \tag{A-16}$$

where the dimensionless groups are

$$N_1 = \frac{\gamma}{KC_\infty l} \tag{A-17}$$

$$N = \frac{KM_1}{RT}\left[\frac{\dot{V}(H_o)}{2l^4} + \frac{\gamma V_o}{KC_\infty l^4}\right] \tag{A-18}$$

The length l characterizes diffusion, it is of the order of several pore lengths and in general $N_1 = O(10^{-3})$, since $KC_\infty = O(10^3\text{psi})$. It is also easily shown that the term N is in general dominated by the volume-curvature derivative $\dot{V}(H_o)$, thus it has its sign. Note that $\dot{V}(H_o) > 0$ (< 0) implies that the equilibria interfaces reside on converging (diverging) pores.

For the solution of (A-12)–(A-16), we consider normal modes

$$\sigma = e^{\omega\tau}\Sigma \tag{A-19}$$

$$\eta = e^{\omega\tau} \tag{A-20}$$

that yield

$$\nabla^2\Sigma = \omega\Sigma \tag{A-21}$$

$$\Sigma \rightarrow 0 \text{ at } \infty \tag{A-22}$$

$$\Sigma = N_1 > 0 \text{ at interface} \tag{A-23}$$

$$N\omega = \int_{\mathcal{A}} \underline{s}\cdot\nabla\Sigma \mid_{\mathcal{A}} dA \text{ at interface} \tag{A-24}$$

$$\underline{s}\cdot\nabla\Sigma = 0 \text{ at pore walls} \tag{A-25}$$

This is an eigenvalue problem for ω, the particular solution of which will not be presented here. For our purposes, it suffices to prove a less general, but nevertheless useful result, that a necessary condition for instability $(\omega > 0)$ is that $N < 0$, which thus implies that configurations with $N > 0$ are stable. Since the sign of N practically coincides with that of $\dot{V}(H_o)$ it follows that equilibrium interfaces resulting into $\dot{V}(H_o) > 0$ are stable to mass transfer.

The proof applies to either a "gas bubble" or a "liquid drop" and proceeds as follows. We multiply (21) by Σ, integrate over the liquid volume and use simple identities to write

$$\int_V \nabla\cdot(\Sigma\nabla\Sigma)dV = \int_V (\mid\nabla\Sigma\mid^2 + \omega\Sigma^2)dV \tag{A-26}$$

Applying Green's theorem on the LHS

$$-\int_{\mathcal{A}} \Sigma(\underline{s}\cdot\nabla\Sigma)dA = \int_V (\mid \nabla\Sigma \mid^2 + \omega\Sigma^2)dV \tag{A-27}$$

and in view of (A-23,A-24), further yields

$$\int_V (\omega\Sigma^2 + \mid \nabla\Sigma \mid^2)dV = -\omega N N_1 \tag{A-28}$$

For $\omega > 0$ it is then necessary that $N < 0$, as claimed. Furthermore, the interesting result also arises that for neutral stability ($\omega = 0$), N must be unbounded,

$$\omega N \rightarrow -\text{constant}$$

Infinitely large and negative N values are obtained for configurations at the extrema of a V vs. H curve (equivalently an r vs. V curve as in Figure 2).

APPENDIX B

Consider the immiscible displacement of an incompressible liquid by the injection of an inviscid gas at variable volumetric rate Q and constant pressure P_G at a point source. At creeping flow conditions, the liquid pressure is typically taken to satisfy a Laplace equation

$$\nabla^2 P = 0 \tag{B-1}$$

$$P_L = P_i \text{ at } \underline{r} \rightarrow \infty \tag{B-2}$$

Locally, at the advancing gas interface we have

$$P_G = P_L + 2\gamma H \tag{B-3}$$

and a growth condition

$$u_s = -\frac{k}{\mu}\frac{\partial P_L}{\partial s} \tag{B-4}$$

where $\underline{s}$ is the local outer normal and Darcy's law has been used to approximately relate velocity and pressure gradient. An overall balance for the gas phase growth reads

$$\frac{d}{dt}[\rho_G V] = \rho_G Q \tag{B-5}$$

which, in case of not-too-large variations in pressure becomes

$$\frac{dV}{dt} = Q = \int_A u_s dA \tag{B-6}$$

Note that the second equality in (B-6) is a direct consequence of Reynolds Transport Theorem.

We shall, next, reduce the problem into a dimensionless form by normalizing spatial distance by an initial gas phase radius R_o, time by $R_o^2\mu/(P_G - P_i)k$, velocity by $(P_G - P_i)k/R_o\mu$, gas volume by R_o^3, interfacial area by R_o^2, and interfacial curvature by H_o (again not necessarily related to R_o). Dimensionless liquid pressure is further defined by

$$\Lambda = \frac{P_G - P_L}{P_G - P_i} \tag{B-7}$$

to yield

$$\nabla^2\Lambda = 0 \tag{B-8}$$

$$\Lambda = 1 \text{ at } \underline{r} \to \infty \tag{B-9}$$

while at the interface we get

$$\nu_s = \frac{\partial\Lambda}{\partial s} \tag{B-10}$$

$$\Lambda = \Psi\eta \tag{B-11}$$

where $\Psi = 2\gamma H_o/(P_G - P_i)$. The dimensionless volume Υ also satisfies the equation

$$\frac{d\Upsilon}{d\tau} = \int_A \frac{\partial \Lambda}{\partial s} dA \tag{B-12}$$

while the latter also equals $Q\mu/\Delta P R_o k$.

Table 1. Typical Values of Parameters

D	10^{-5} cm^2/sec
H_o^{-1}	50 μm
k	1 darcy
K	3.75×10^4 psi/gr/cm^3
M_1	20 gr/mol
P_b	2000 psi
T	30 °C
γ	30 dynes/cm
μ	10 cp
ρ	0.8 gr/cm^3

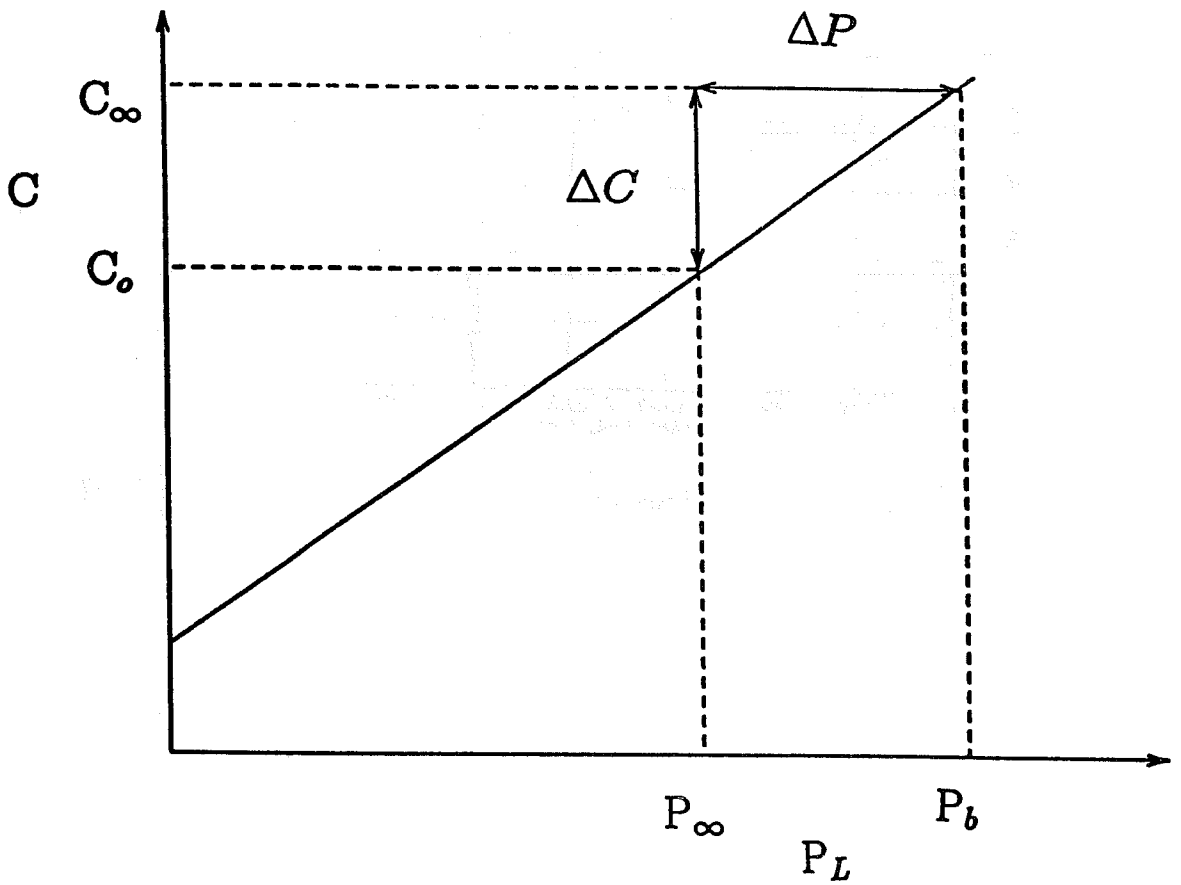

Figure 1a. Gas solubility vs. pressure schematic.

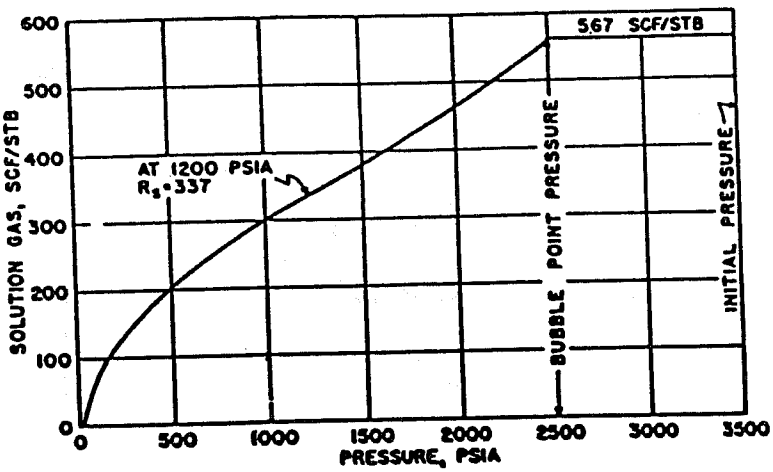

Figure 1b. Typical solution gas-oil ratio vs. pressure [44].

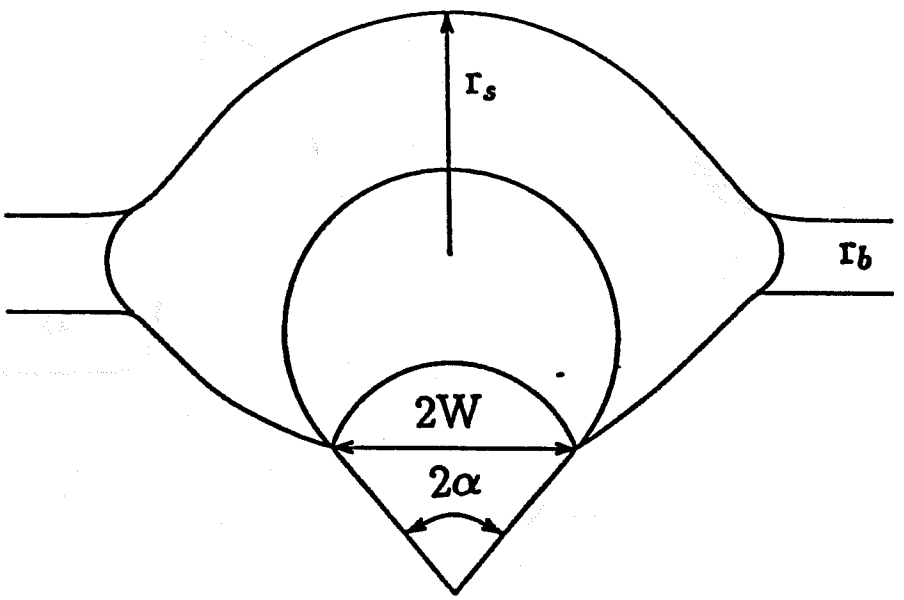

Figure 2a. Schematic of a nucleation site in a host pore body.

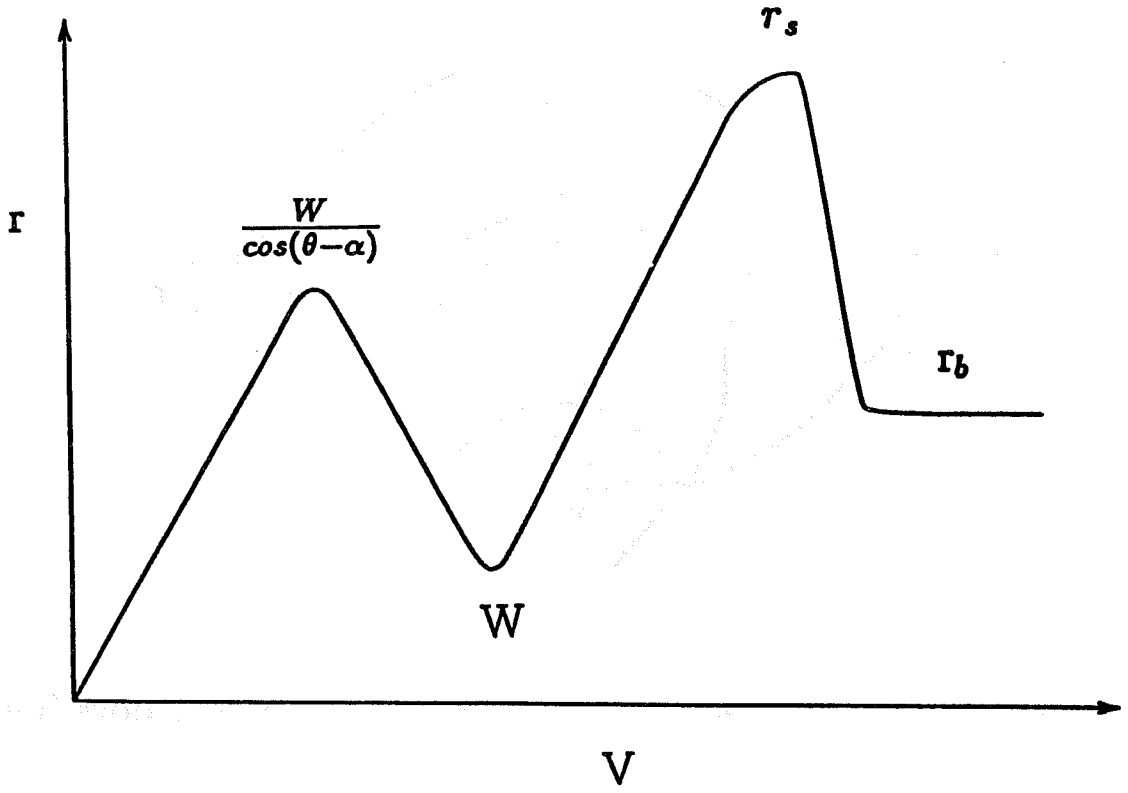

Figure 2b. Schematic of bubble radius-volume relationship.

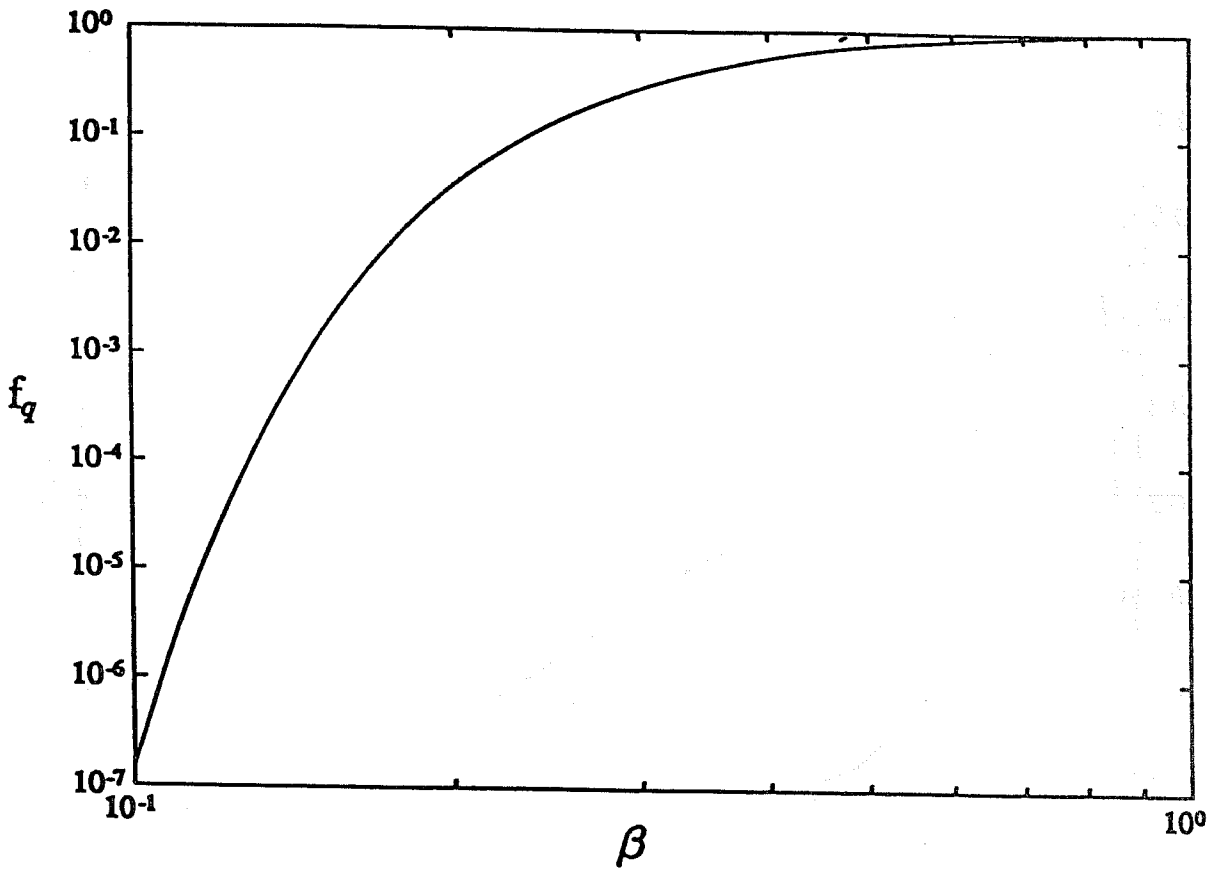

Figure 3a. Nucleation fraction at threshold vs. β (Z=6).

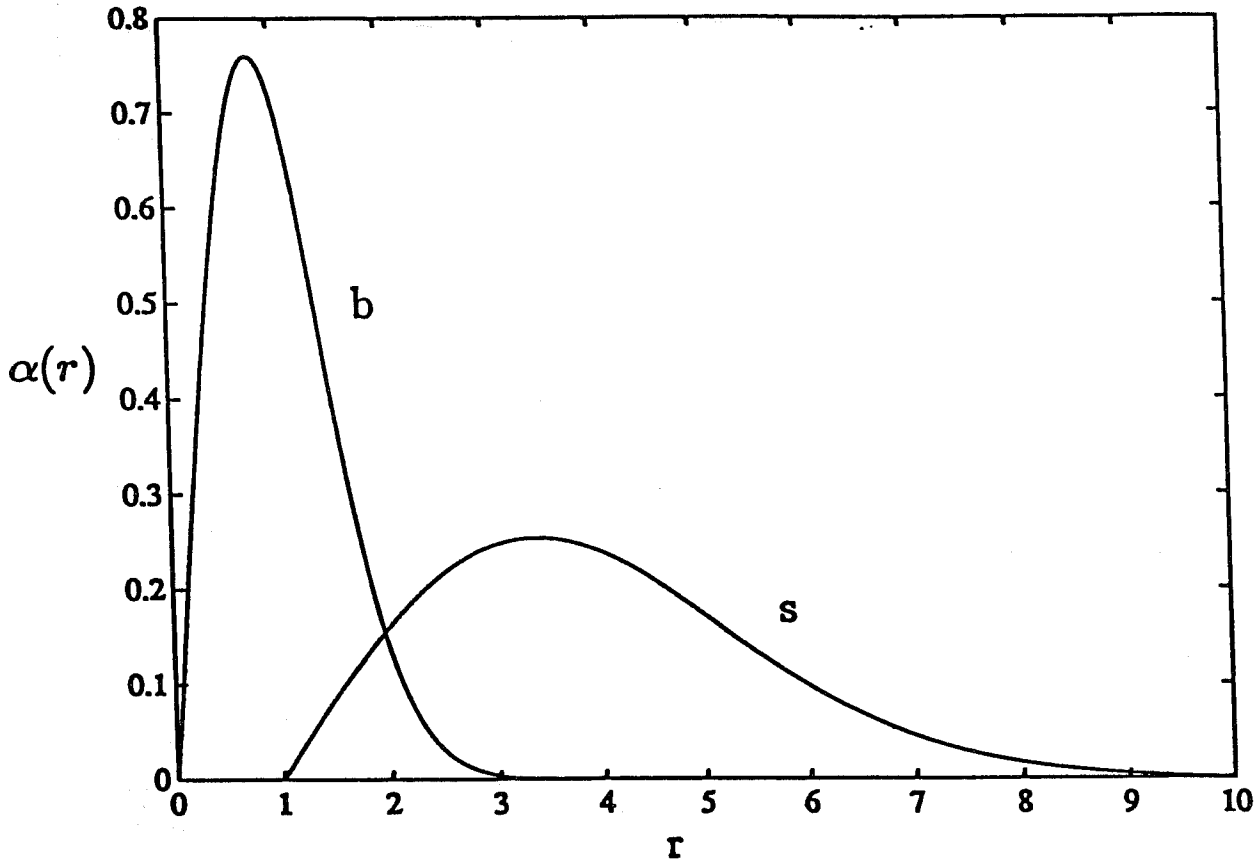

Figure 3b. Pore body and pore throat size distributions.

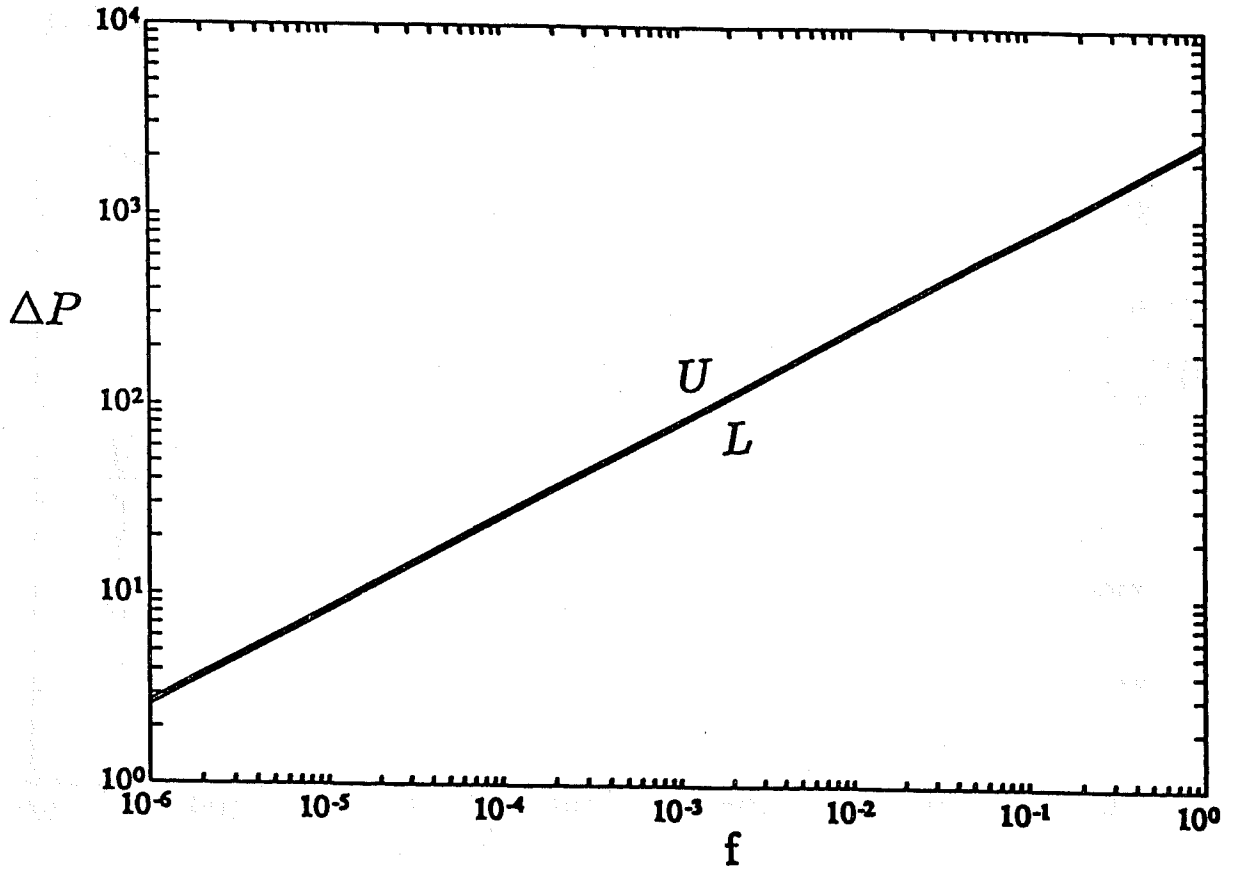

Figure 4a. Critical supersaturation vs. f for various decline rates: $a = 1$ (U), $a = 10^{-4}$ psi/sec (L).

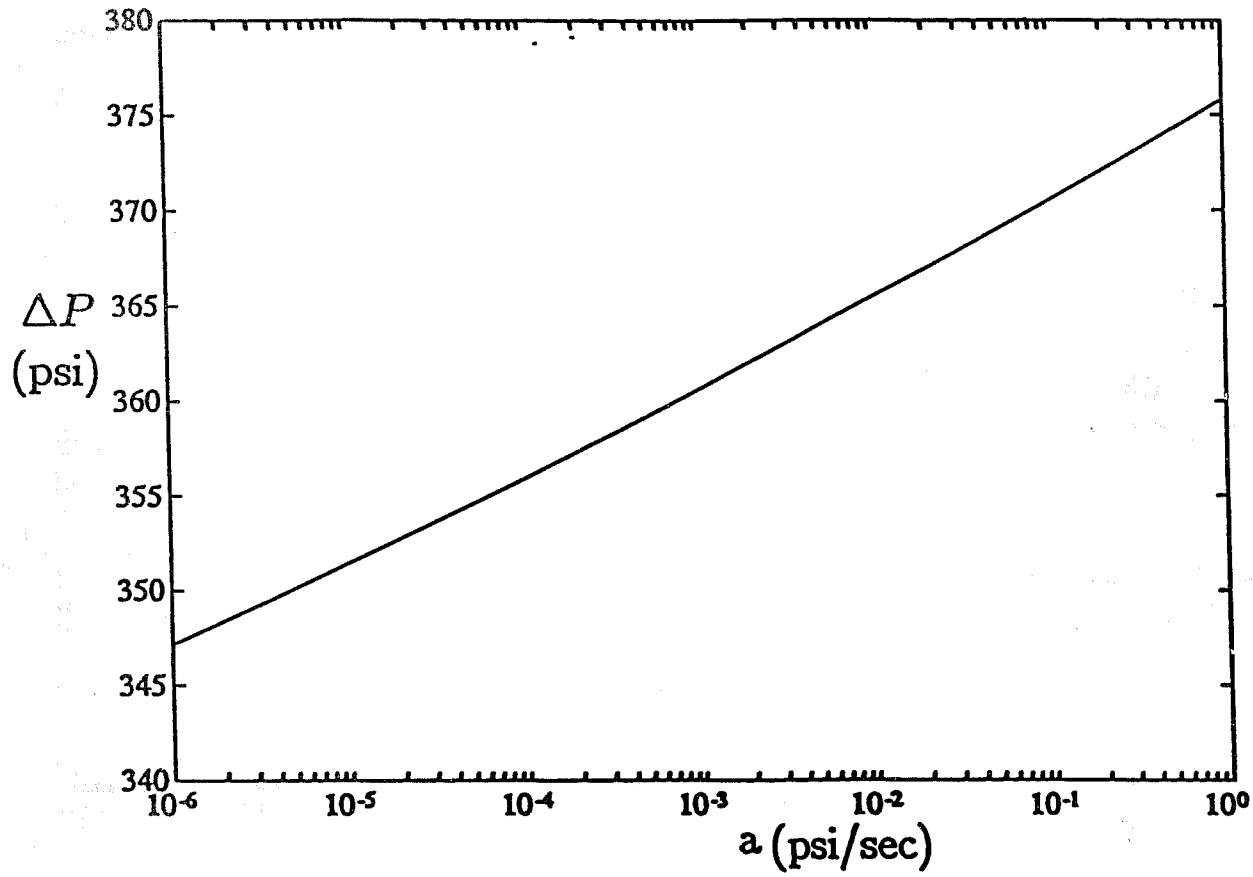

Figure 4b. Critical supersaturation vs. pressure decline rate for f=0.1.

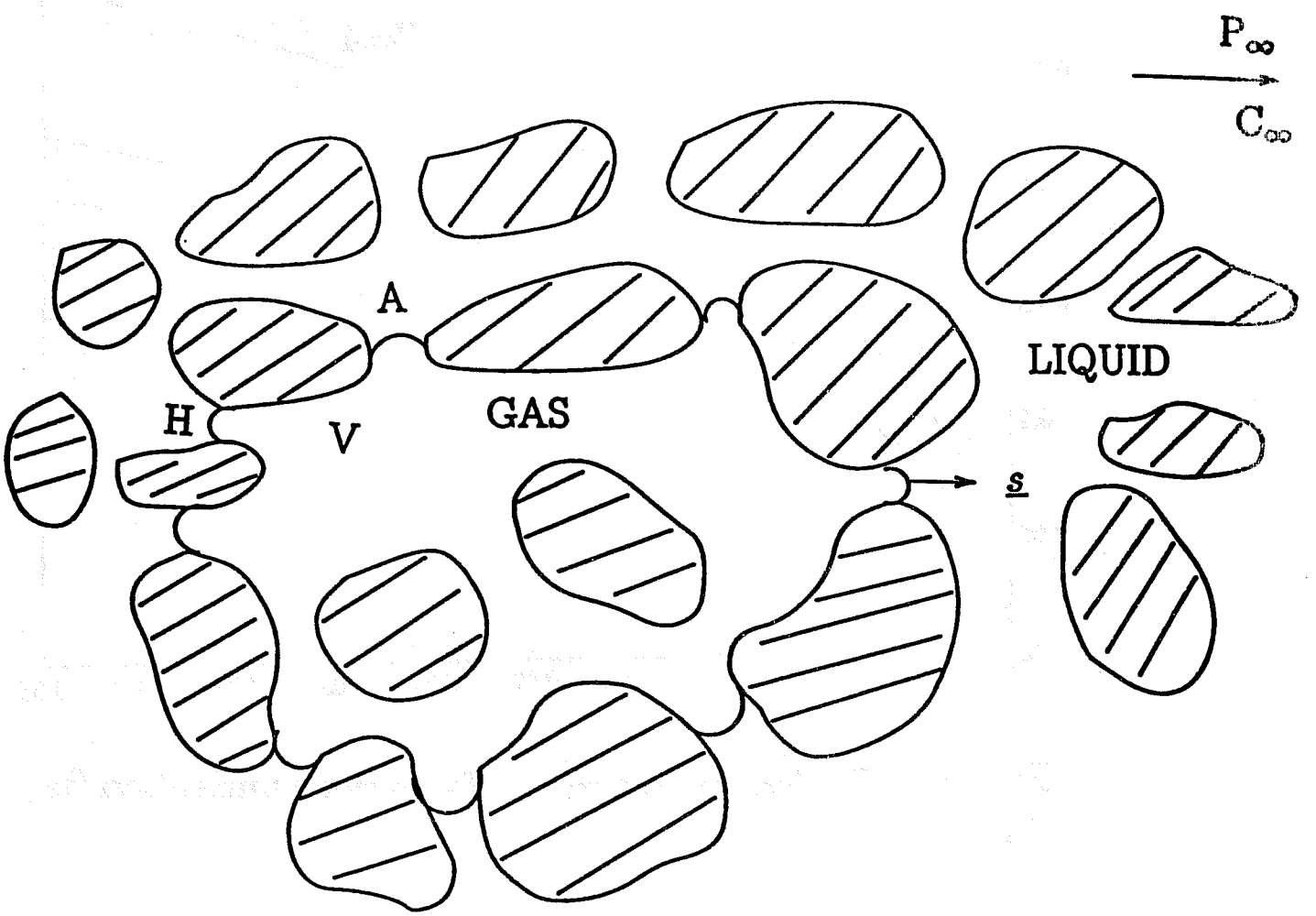

Figure 5. Schematic of a gas bubble in a porous medium.

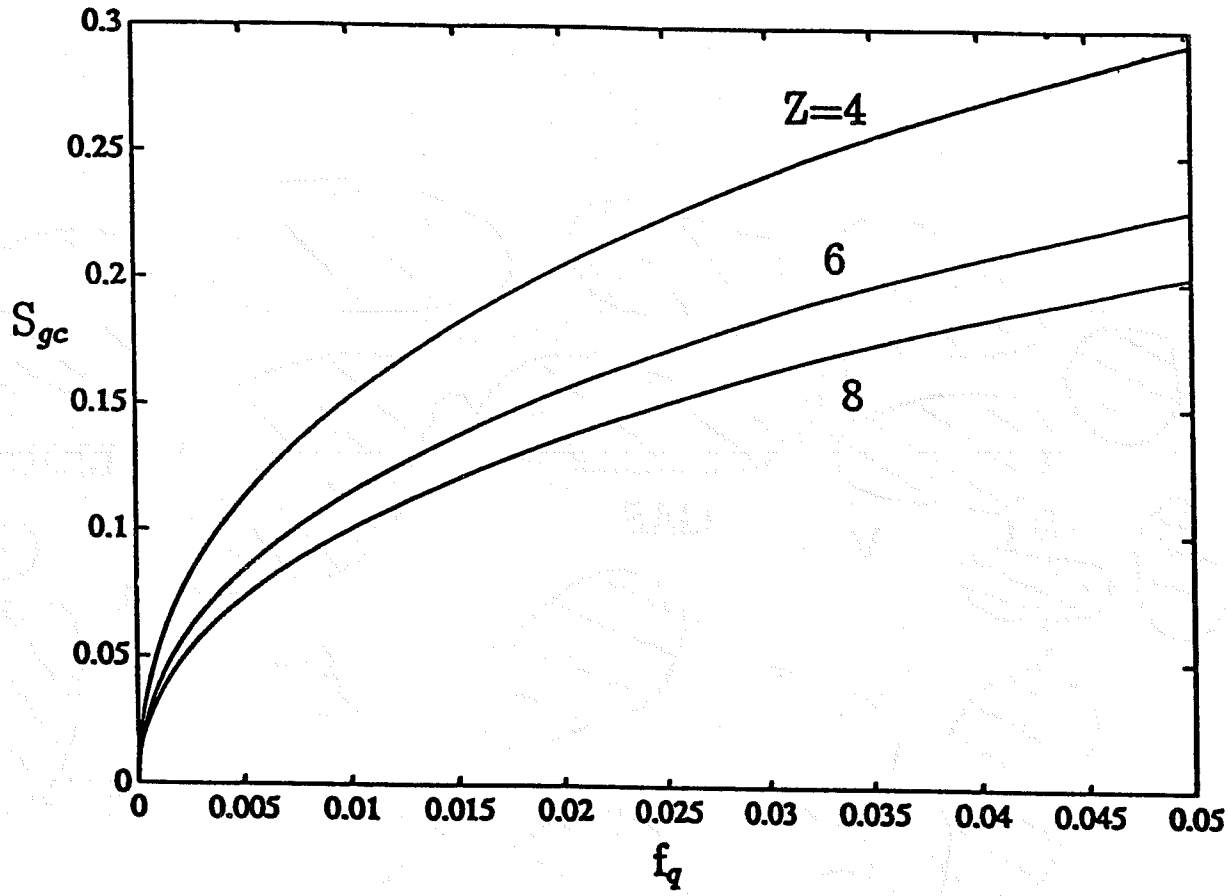

Figure 6. Critical gas saturation for various nucleation fractions.

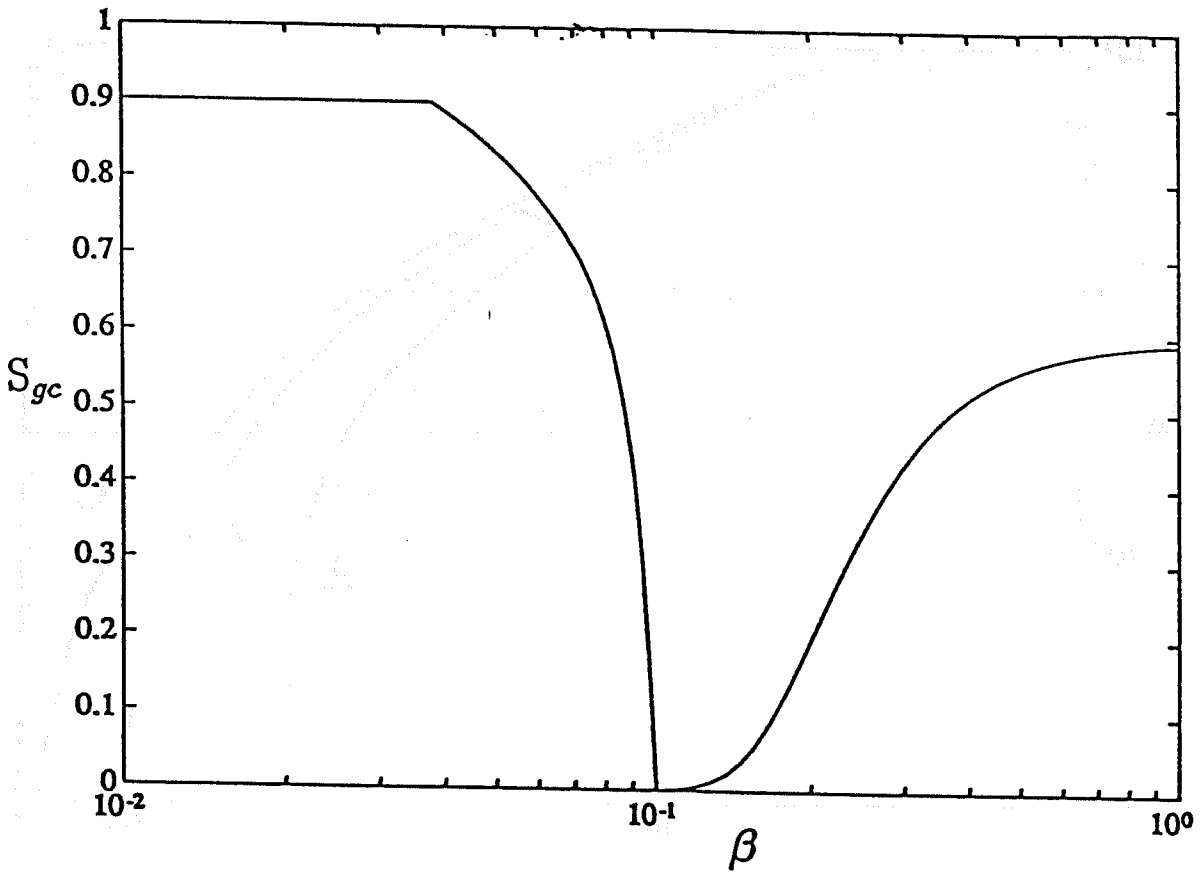

Figure 7. Critical gas saturation as a function of β (κ=0.1).

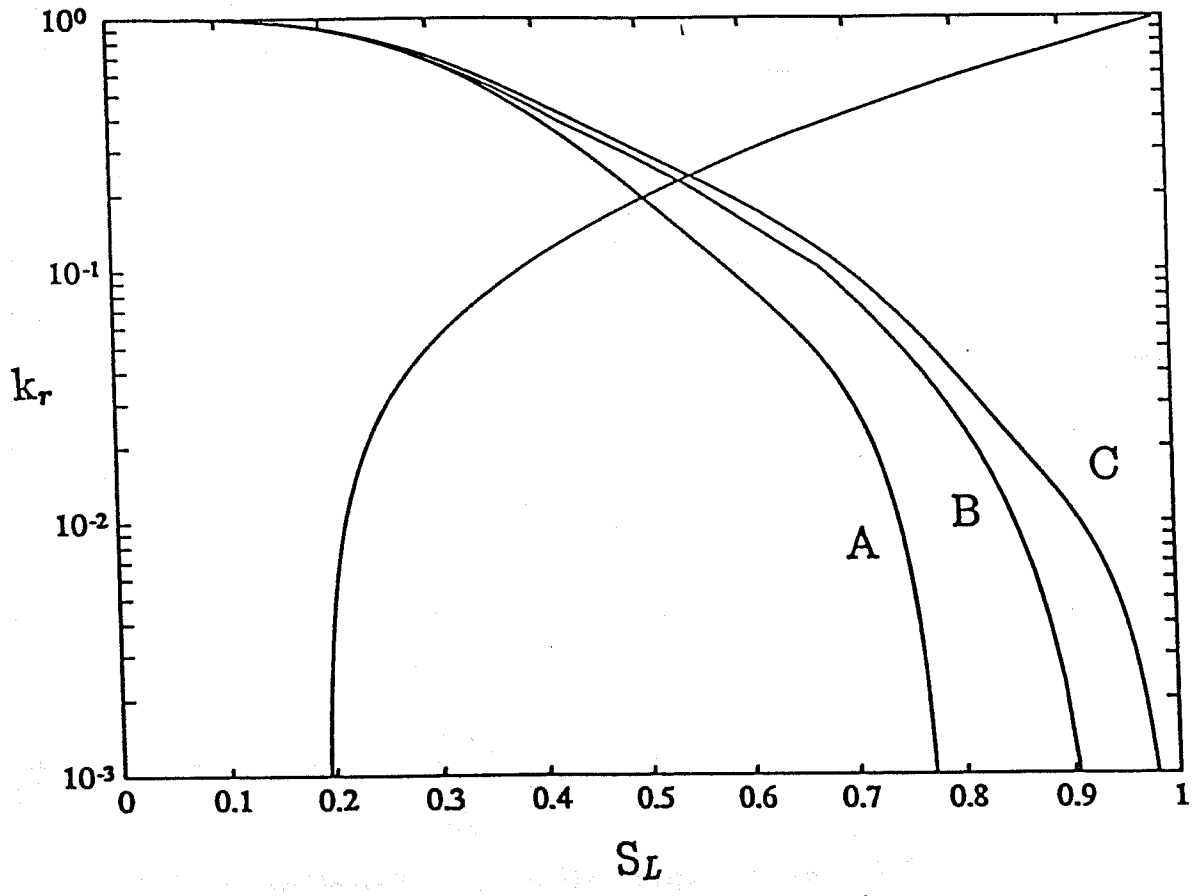

Figure 8a. Internal (A,B) and external (C) gas drive relative permeabilities, β=0.20, 0.16, 0, respectively (Z=6).

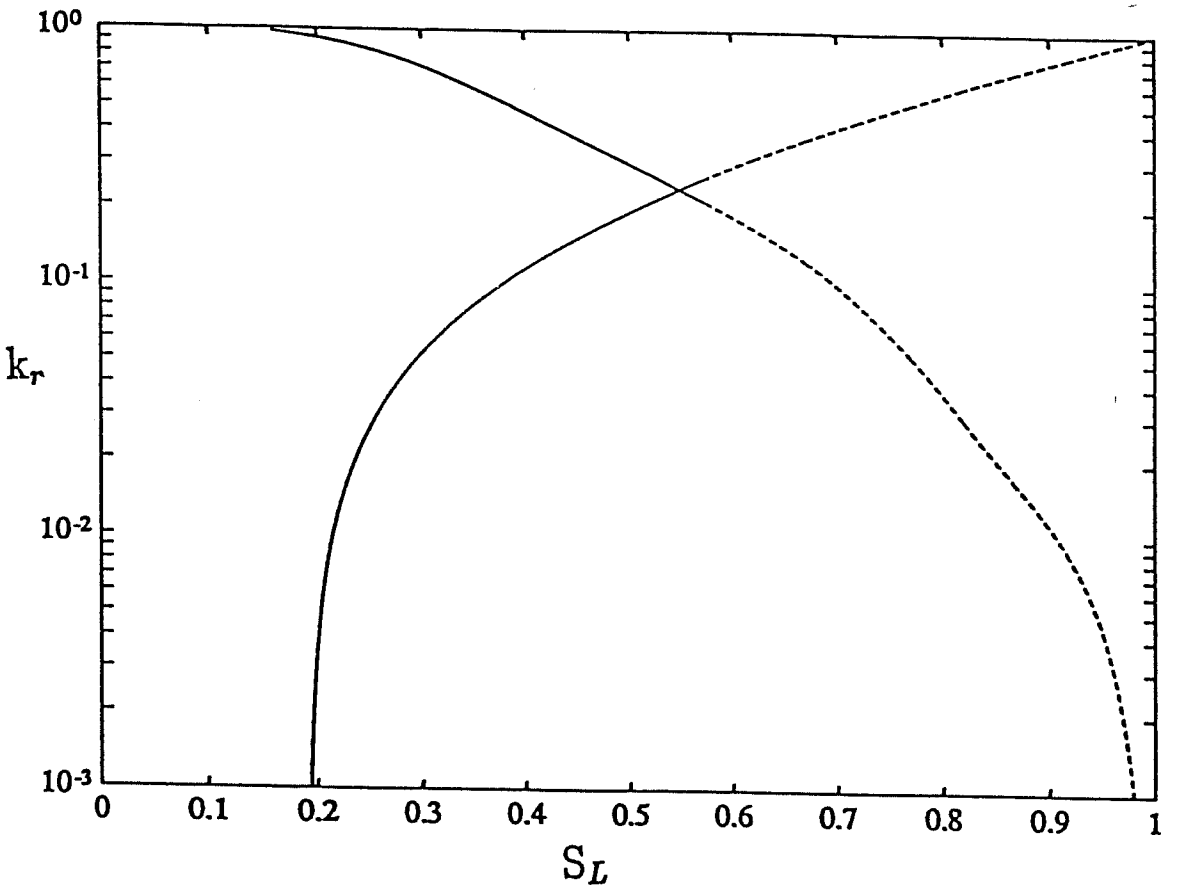

Figure 8b. Internal gas drive relative permeabilities (Z=6, β=0.09, κ=0.1).
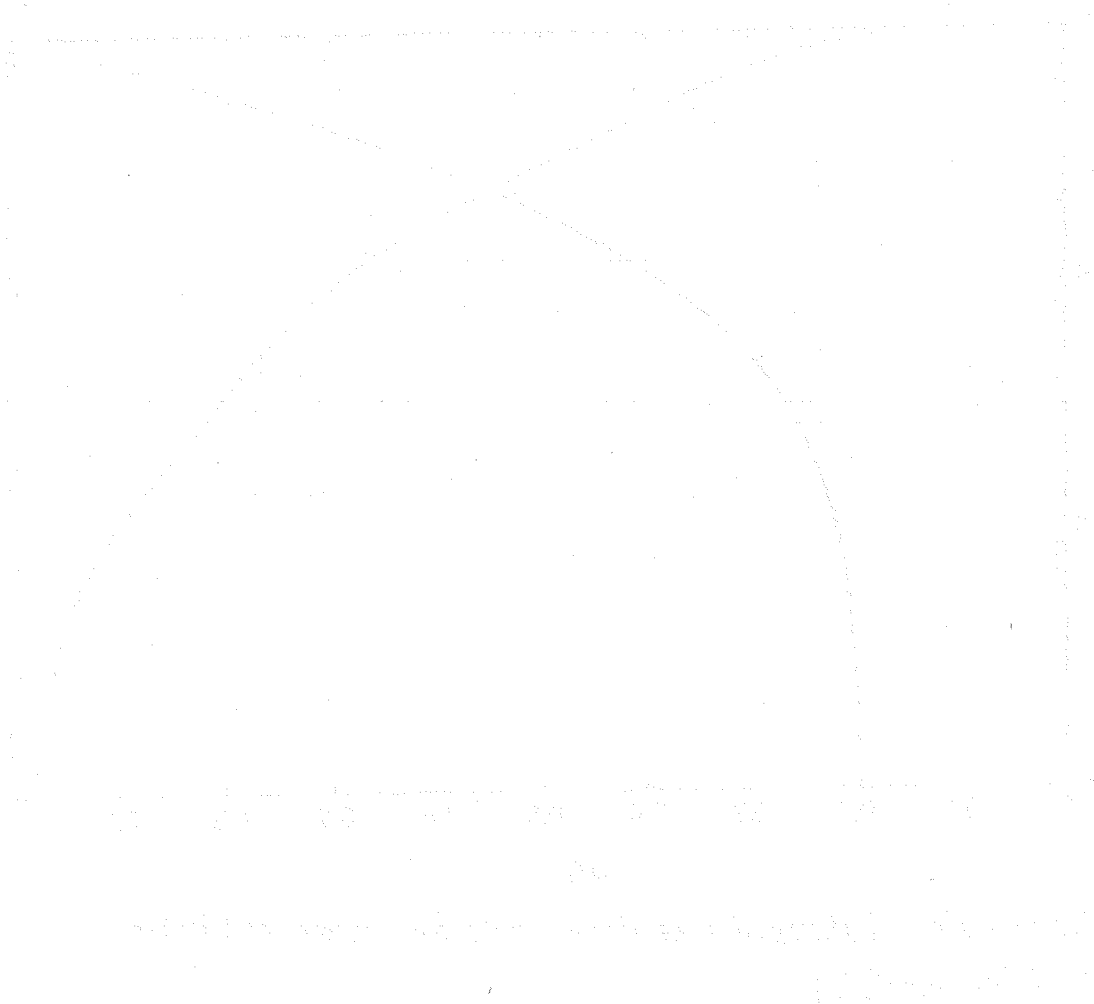
☆U.S. GOVERNMENT PRINTING OFFICE: 1989-661-023/00044